Final Response to referees - Intermittency of Arctic-midlatitude teleconnections: stratospheric pathway between autumn sea ice and the winter NAO

Peter Yu Feng Siew, Camille Li, Stefan Pieter Sobolowski, and Martin Peter King

Anonymous Referee #1

The authors have examined in great detail the causal linkage between autumn Barents-Kara Sea ice anomalies and winter surface climate. The paper is well written and the logic is sound.

We would like to thank the reviewer for the comments. We have provided a point-by-point response to the comments below. Reviewers' comments are in blue, our initial responses are in black and responses related to the revised manuscript are in red.

1. A piece of potentially useful information missing is why November is selected as the source timing and February as the resulting timing, given that October Barents-Kara Sea ice is even better correlated with January NAO variability than the November sea ice - February NAO counterparts. In addition, NAO variability is larger in January than in February, which makes better sense to explore the October-January pathway.

In the CEN analysis, we do not select specific pathways between specific months, but rather allow the CEN algorithm to objectively identify causal linkages that make up pathways. In the monthly CEN (Fig. 2a and Fig. S1a in the submitted manuscript), the stratospheric pathway does in fact originate with October Barents-Kara sea ice. In the half-monthly CEN (Fig. 2b and Fig. S1b in the submitted manuscript), a pathway from November Barents-Kara sea ice to January NAO does appear (consistent with some previous studies), although it does not go through the stratosphere, which is the focus of this study. Fig. 1 shows simple lagged correlations between October and November Barents-Kara sea ice indices, and NAO from October to February. We can see that the ICE_{Oct}-NAO_{Feb} and ICE_{Nov}-NAO_{Jan} correlations are the strongest, and it is in fact these pathways that the CEN picks. There are also quite strong correlations between ICE and December NAO, but these are not part of any connected pathways identified by the CEN analysis. This could be due to the fact that these correlations are not stationary in time, and depend on the exact reanalysis period used (also discussed in Introduction of submitted manuscript and mentioned below in point #2).

Please see lines 193-196 and Fig. S5 in the revised supplement.

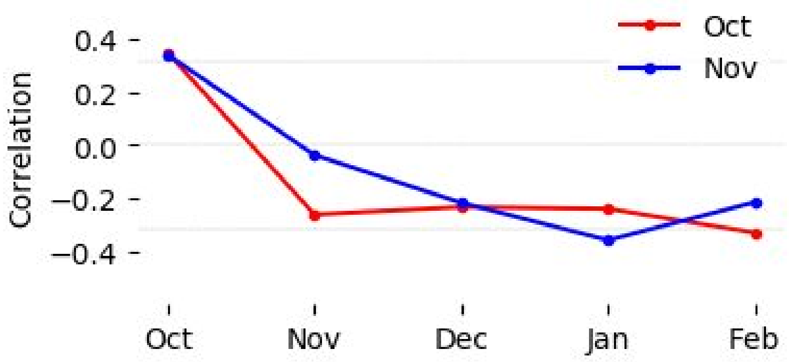

Fig. 1: The correlation between October (red) and November (blue) Barents-Kara sea ice indices, and NAO from October to February. Outer grey lines show significant correlations at a 5% level using a two-tailed t-test.

2. In addition, the sea ice-NAO linkage is sensitive to the investigation period, i.e., 1979-2010 vs 1979-2018 as in Fig.1. There seems to be a few possibilities that might explain such non-robustness. For example, the time it takes from the sea ice to the NAO might vary in different periods (not always being three months). Alternatively, the timing might shift over time, e.g., due to changes in the seasonal cycle of the stratospheric jet strength in response to anthropogenic forcing.

We agree that there are a number of factors that may contribute to the non-robustness of the linkage. The non-stationarity of the pathway's timing certainly might be one of them. While a comprehensive investigation into all the possible mechanisms is beyond the scope of the paper, we do make an effort to discuss what we feel are some prime candidates.

In the revised manuscript, we will expand the discussion, including a mention of the timing issue raised here, and also mention the influence of anthropogenic forcing on the seasonal cycle of the stratosphere as possible sources of intermittency.

Please see lines 39-41 and lines 339-341.

Anonymous Referee #2

General Comments: The present manuscript discusses the potential link between Barents and Kara sea ice in autumn and the late winter NAO via the so-called "stratospheric pathway. By applying a causal effect network (CEN) approach, the authors focus on the intermittency of the pathway and discuss the role of both sub-seasonal and synoptic processes. The manuscript is well written and structured and the results are presented in a balanced way and discussed in the context of the relevant literature. Overall, I find the analysis a valuable contribution to the ongoing debate about Arctic-mid-latitude linkages, highlighting the importance of different time-scales and potential non-stationarities as well as the need for statistical concepts to deal with these challenges. I do have some comments which I think would improve the manuscript. In particular, the significance testing of the CEN analysis is not optimal and the regression analysis seems to lack some consistency with the CEN analysis. The results of the "Synoptic linkages and interactions across times scales" section on the other hand deserve more weight in my opinion as they are a novel attempt to explain non-stationarities of the stratospheric pathway and might be an important step towards reconciling model and observation analyses.

We would like to thank the reviewer for the supportive comments and suggestions for improvement. We have provided a point-by-point response to the specific comments below. Reviewers' comments are in blue, our initial responses are in black and responses related to the revised manuscript are in red.

1. I am well familiar with the applied method and am certainly convinced by its advantages and thus also pleased to see it being used. Nevertheless, I think that the authors do not apply it an optimal way. Since Kretschmer et al. (2016) and Runge et al. (2014) there have been several advancements to this approach as discussed in more detail in Runge et al. (2019, which was published after the authors submission) and Kretschmer et al (2018, npj) and Runge et al. (2018, Chaos). In particular the authors do not adequately account for the issue of multiple testing and false positives: They only test links found in their step 1 (the correlation analysis)

and then use partial correlation tests to check if the correlation from step 1 can be explained by confounders. Due to the involved multiple testing (in step 2) of links, the significance level alpha cannot be interpreted as the false positive rate. The authors, however, use this alpha level for further interpretations of their results. Note that this can be overcome by considering their step 1+2 only as a "condition selection step" and then testing each possible link again using partial correlations with the conditions identified before (as described in detail in Runge et al. 2019). Not only does this yield in more statistical interpretability but, furthermore, this can also lead to higher detection power. The reason is that a true link A->B can be overlooked because correlations are zero (see C2 WCDD Interactive comment Printer-friendly version Discussion paper their step 1) but conditioning out the influence of a common driver C (with opposite effects on A and B) reveals the actual signal (which might also affect the intermittency statistics). In this context, also note that estimating this condition set for each variable can be done by using different and rather liberal alpha levels (considered as a hyperparameter or a significance "threshold") and the "optimal" set can then be chosen, for example, based on the Akaike information criterion (AIC), as described in Runge et al. 2019. Further, the authors should be aware that the overall resulting network is also subject to the "field significance" issue (see e.g. Wilks 2017, BAMS). This means that just by chance, some of the detected significant links will be false positives. This can also be addressed by applying false discovery rate corrections to the overall network. This issue might not be too relevant for the monthly CEN which only consists of few links, but might be an issue for the synoptic-scales CENs. That said, I don0 t expect the authors to include all these novelties in their approach. Nevertheless, these issues should be discussed properly and the parts where referred to significance should be adapted. Further, I don't agree with their statement in l 136 that testing each link again in step 2 of the analysis in Kretschmer et al (2016) is "somewhat arbitrary". On the contrast, it is one way to deal with multiple testing problem as described above. Maybe the authors also want to consider comparing their results with the pcmci implementation provided here https://github.com/jakobrunge/tigramite/

Thank you for informing us about the latest publications and advances in the CEN approach. We agree that the CEN algorithm used in the submitted manuscript is not complete. We tested many of the suggested CEN modifications and redid our analyses accordingly - while the main results do not change, there are a number of aspects detailed here that we feel are worth including in a revised manuscript.

We have now adopted two modifications to improve the CEN method. Firstly, the Akaike information criterion (AIC) is used to select the optimal condition set of each variable in the PC step (following terminology in Runge et al. 2019), with significance levels set at 0.05, 0.1 and 0.2. Secondly, the MCI test is introduced, whereby we test each possible link again using partial correlations with the conditions identified in the PC step.

Fig. 3 shows the stratospheric pathway in the (a) monthly and (b) half-monthly CEN using the modified algorithm. Some new linkages appear as a result of the higher detection power with the MCI step. The monthly CEN detects an additional branch of the stratospheric pathway which links $URALS_{Dec}$ to NAO_{Mar}. In the half-monthly CEN, a few more linkages (e.g., $THF_{Nov} \rightarrow SPV_{Dec}$ and $V^*T^*_{Jan} \rightarrow NAO_{Feb}$) are detected, but they do not change the results in terms of overall pathways. The intermittency rates of individual segments in the original $ICE_{Oct} \rightarrow NAO_{Feb}$ pathway do not change significantly (Fig. 3). The full stratospheric pathway now appears in 16.5% (compared to 15% before) of bootstrap samples.

In addition, we performed several other sensitivity tests on the algorithm:

- In the PC step, we used the Akaike Information criterion (AIC) to select the optimal significance level for individual variables in individual months, with three significance level sets: 0.05, 0.1, 0.2 (Fig. 2); 0.05, 0.1, 0.2, 0.3 (Fig. 4a); 0.05, 0.1, 0.2, 0.3, 0.4, 0.5 (Fig. 4b). The stratospheric pathways in the monthly CEN are unchanged in all sets. The pathways in the half-monthly CEN change slightly using the second and third sets. With the inclusion of less strict significance levels at which (partial) correlations are deemed not significant, more parents are identified in the PC steps. This leads to higher dimensionality in the MCI step, which means that causal linkages are rejected more easily (e.g., disappearance of the $SPV_{Jan} \rightarrow NAO_{Feb}$ in Figs. 4a & 4b). Because our focus is the monthly CEN, we prefer to use the significance set 0.05, 0.1, 0.2, which produces consistent pathways in the half-monthly CEN as well, but we will discuss the sensitivity of the half-monthly results to this analysis choice.
- We performed a quick test applying the Hochberg-Benjamini false discovery rate (FDR) control to adjust the p-values in the MCI test, although the reviewer felt that this refinement was less important than others. This approach greatly reduces the number of detected linkages (Fig. 5). One problem we had was in determining the number of independent tests m to calculate the adjusted P-value = P*m/r, where P is the original P-value and r is the rank of the original P-value (sorted in ascending order). We used m=360 here (5 months * 6 variables* 6 variables * 2 lags), but these 360 tests are not truly independent, given the strong autocorrelation in many of these variables. We are not able to find a straightforward way to deal with this, and are inclined to leave out this FDR step.

In the revised manuscript, we will modify the Methods section to describe the modifications to the algorithm, primarily the MCI and the AIC. Results and the discussion will be revised to account for the new results. Since the conclusions drawn from the new results are consistent with the previous results, there will not be any significant changes to the main messages. We do agree with the reviewer that the phrase “somewhat arbitrary” in L136 was poorly worded. We will delete this sentence since we now include the MCI test.

Please see lines 104-151, and Figs. 3, 5, 6 and 7 and S1-S9 in the revised manuscript and supplement.

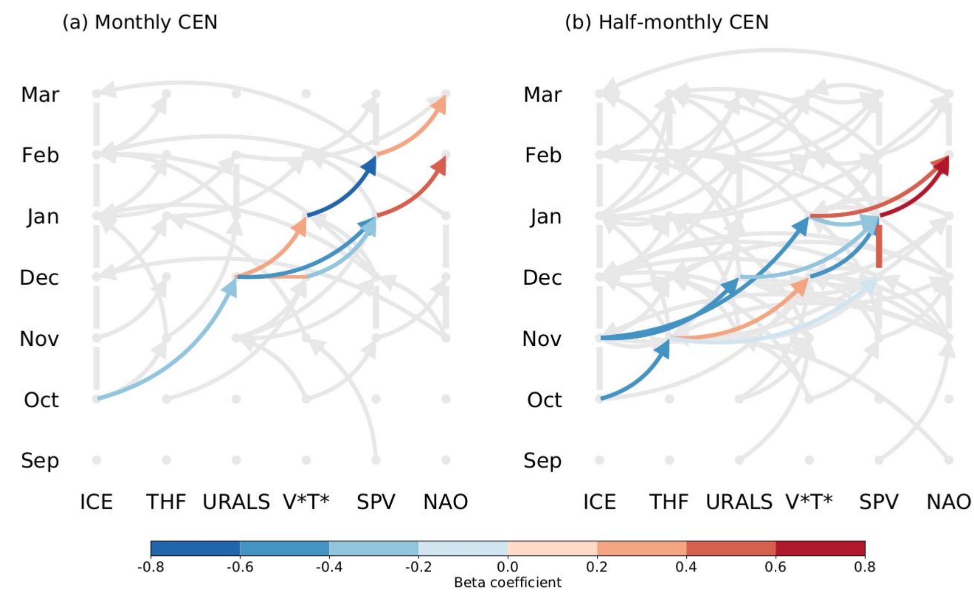

Fig.2 : As in Fig. 3 in the submitted manuscript, but using the modified CEN algorithm (with the

addition of the AIC with significance set 0.05, 0.1, 0.2 and the MCI test).

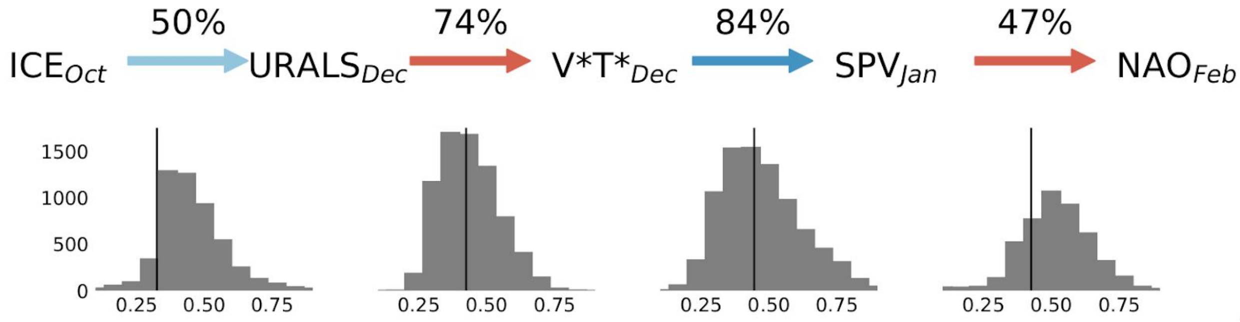

Fig. 3: As in Fig. 4 in the submitted manuscript, but using the modified CEN algorithm.

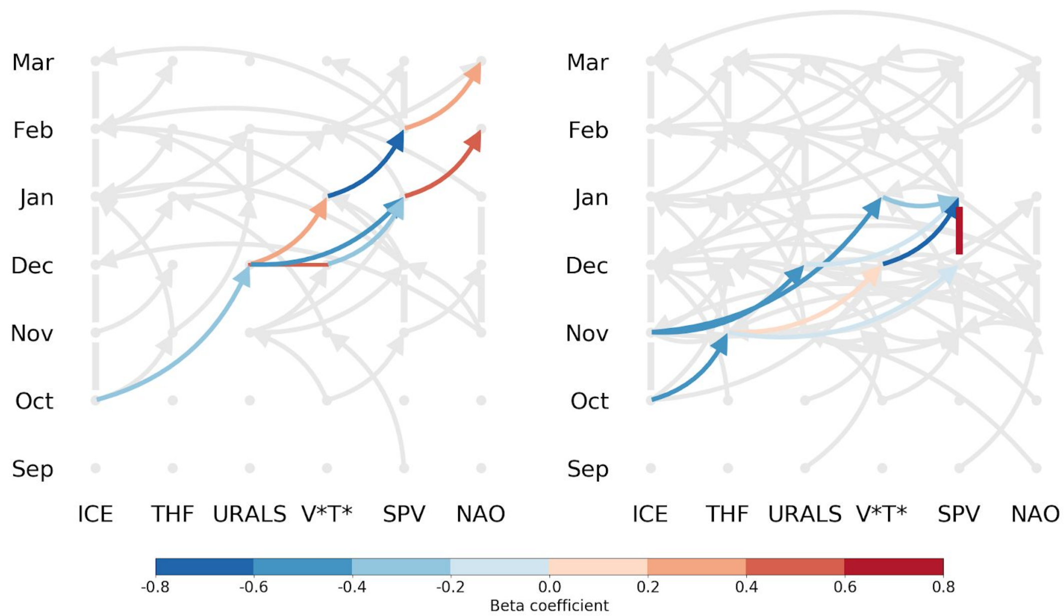

Fig. 4a: As in Fig. 2, but using AIC with significance set 0.05, 0.1, 0.2, 0.3.

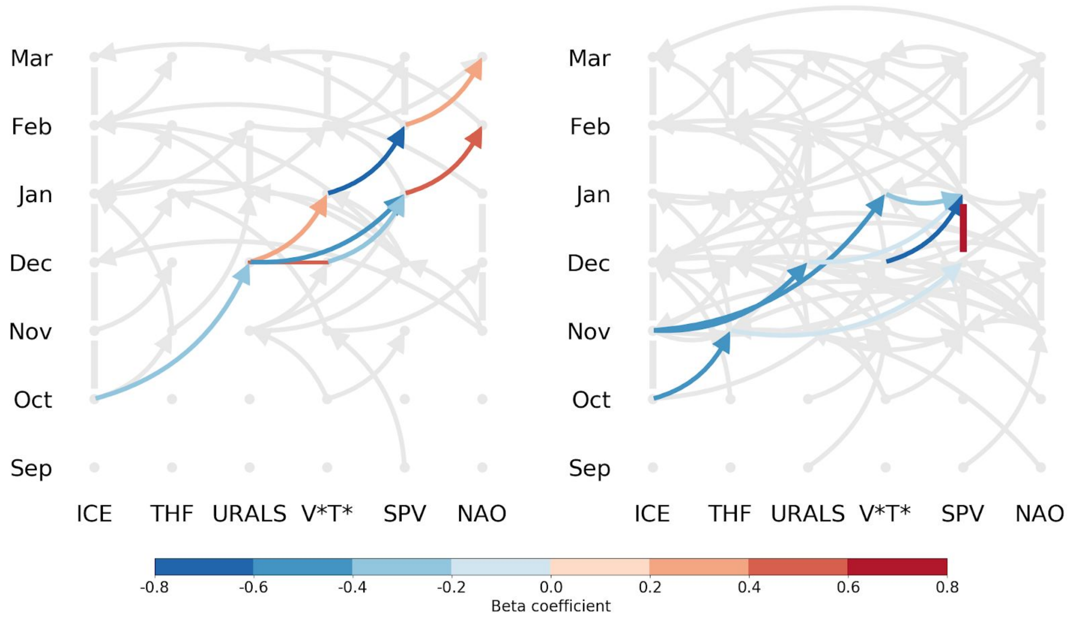

Fig. 4b: As in Fig. 2, but using AIC with significance set 0.05, 0.1, 0.2, 0.3, 0.4, 0.5.

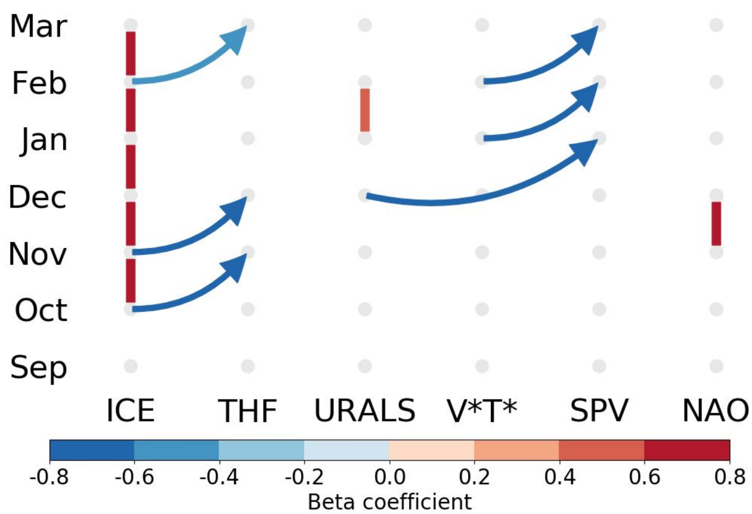

Fig. 5: As in Fig. 2a, but with the application of the False Discovery Rate correction using m=360.

2. Strength of the pathway. When estimating the influence on NAO variability, the regression analysis seems somehow contradictory to the previous analysis. Why would one include the whole pathway if one believes that it represents an indirect chain of links? More precisely, if, for instance, the influence of BK SIC on SPV is via Urals then, in theory, the whole information is already contained in Urals and adding BK SIC in the regression should not provide additional information. Following the logic of a network, the causal effect from A–>B is the sum over the products of link coefficients along all possible paths between the two variables (see for example here: https://github.com/jakobrunge/tigramite/blob/master/tutorials/tigramite_tutorial_causal_effects_

mediation.ipynb). Also, it seems obvious that adding more regressors to the regression analysis also increases its r2? Is the analysis performed for all years? Wouldn't it make sense to use a similar bootstrap approach or at least some leave-k-out cross validation? As stated before, a more interesting analysis could be an attempt to quantify the contribution of sea ice to the NAO via the tropospheric and via the stratospheric pathways alone. This recent paper might me an interesting source of inspiration how do approach this using the CEN approach: Saggioro, E. and Shepherd, T. G. (2019) Quantifying the timescale and strength of Southern Hemisphere intra-seasonal stratosphere-troposphere coupling. Geophysical Research Letters. ISSN 0094-8276

Thank you for these comments. One purpose of this analysis is to carry out a simple assessment of the strength of the pathway as observed within the whole satellite period, using all years (1979-2018) without resampling. This analysis shows that the pathway can explain 26% of the interannual variability in $NAO_{Feb.}$ We agree that it is a bit confusing to introduce this information at this point of the manuscript. We suggest to streamline the material, and move it earlier in the manuscript - right after the identification of the pathway and before the intermittency test to achieve better logical flow.

In response to the reviewer's other concerns/questions: Yes, adding more regressors will usually increase the variance explained. Our purpose here was to compare this to the other bars in Fig. 5 in the submitted manuscript, to explore how different regression approaches (blue bars showing the effect of individual regressors versus green bars showing the effect of removing individual regressors) gives slightly different views on how the information is passed through the pathway.

As the reviewer suggests, we can quantify the relative contribution of the tropospheric and stratospheric ICE-NAO pathways as in Runge et al. 2015. For example, ICE_{Oct}-NAO_{Mar} (Fig. 6) consists of both tropospheric and stratospheric components. The tropospheric pathway has a mediated causal effect: -0.661 ($ICE_{Oct}\rightarrow THF_{Nov}$) * 0.384 ($THF_{Nov}\rightarrow URALS_{Jan}$) * 0.517 ($URALS_{Jan}\rightarrow URALS_{Feb}$) * -0.468 ($URALS_{Feb}\rightarrow NAO_{Mar}$) = 0.0614; The stratospheric pathway has a mediated causal effect: -0.326 ($ICE_{Oct}\rightarrow URALS_{Dec}$) * 0.368 ($URALS_{Dec}\rightarrow V^*T^*_{Jan}$) * -0.715 ($V^*T^*_{Jan}\rightarrow SPV_{Feb}$) * 0.301 ($SPV_{Jan}\rightarrow NAO_{Mar}$) = 0.0258. Therefore, the tropospheric and stratospheric pathways account for 70.4% (0.0614/(0.0614+0.0258)) and 29.6% (0.0258/(0.0614+0.0258)) of the total causal effect, respectively. It is interesting that the tropospheric pathway is stronger, a point that, to our knowledge, has not been demonstrated previously. The result is perhaps unsurprising, given that the stratospheric pathway is undermined by both noise from the troposphere and noise from the stratosphere. Other pathways exist in the CEN, but we note that it is only meaningful to compare pathways with the same timing in terms of initial and ending months. Saggioro and Shepherd (2019) indeed provide a simple prediction model to quantify the strength of links, but it might be too complicated to apply this in our CEN since we are exploring pathways with multiple linkages.

In the revised manuscript, we will move this material into the end of section 3.1 (before the intermittency analysis), state clearly the purpose of these analyses, and streamline the text. We will also include an evaluation of the relative strength of pathways in terms of the mediated and total causal effects, as described above.

Please see lines 197-223, lines 249-251 and Table 1 in the revised manuscript.

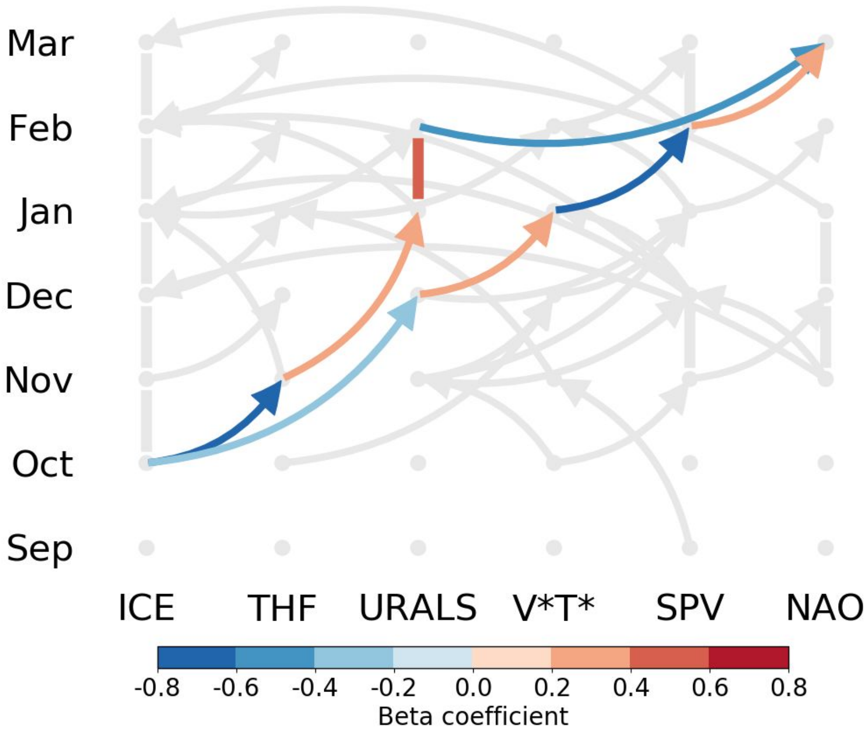

Fig. 6: As in Fig. 2a, but highlighting the $ICE_{Nov} \rightarrow NAO_{Mar}$ stratospheric and tropospheric pathways.

3. Intermittency. Addressing the intermittency of the Arctic – NAO link is very interesting and important given that it might provide an explanation why models and observation studies don't seem to agree on this topic. It is well known that not all extremely weak polar vortex states (or SSWs) affect tropospheric circulation (e.g. Karpechko et al. 2017, Runde et al. 2016). Do I understand the authors correctly that sea ice variability might also contribute to this downward intermittency (for example due to sub-seasonal-synoptic interactions)? I think it would make sense to highlight the intermittency of both the upward and the downward coupling mechanisms separately (with the upward part representing somehow the potential of sea ice to influence the NAO).

Yes, in this section, overall we are trying to make a point that there is quite some intermittency along the entire pathway that could contribute to the disagreement between models and observations, and that this intermittency arises from processes operating at different time scales.

Ice certainly plays a role in the intermittency of these pathways. Fig. 7 in the submitted manuscript breaks the synoptic Arctic-midlatitude interactions into "from Arctic" and "to Arctic" linkages, both of which focus on the upward coupling. The "from Arctic" case primarily shows the linkages ↓ICE→↑IR→↑URALS. In this case, synoptic processes reinforce the upward coupling seen in the monthly and half-monthly CEN. The "to Arctic" case exhibits evidence of large-scale flow conditions favouring moist intrusions or simply moisture transport by cyclones tracking into the Barents (↑URALS→↑IR→↓ICE), which would act as a positive feedback on ice reductions. This means that even if there is low autumn sea ice in a given year, synoptic internal variability (which is large) could create anomalously low SLP over the Urals, leading to negative downward IR anomalies (lack of moist intrusions/cyclones) and positive ice anomalies, thus interrupting the upward coupling.

Pinning down the “source” of the intermittency is actually quite an interesting question. In the ICE_{Oct}→ NAO_{Feb} stratospheric pathway in the monthly CEN, the upward coupling includes the segments ICE_{Oct}→$URALS_{Dec}$ and $URALS_{Dec}$→$V^*T^*_{Dec}$, whose intermittency rates are 50% and 74%, respectively (Fig. 3). The occurrence of these two linkages together is seen in about 41% out of 10,000 bootstrap samples, meaning that most of the time when we have the ICE_{Oct}→$URALS_{Dec}$ linkage, the subsequent link to $V^*T^*_{Dec}$ is also seen. Conversely, only about half of the time that the linkage $URALS_{Dec}$→$V^*T^*_{Dec}$ is detected is it preceded by the ICE_{Oct}→ $URALS_{Dec}$ linkage. It seems most likely that most the intermittency in both segments (individually and in terms of their “combined” occurrence rate) stems from variability in $URALS_{Dec}$ related to atmospheric internal variability.

In the revised manuscript, we will provide a more comprehensive discussion of how to interpret the intermittency analysis, and contrast the roles of different processes in the various pathways connecting ICE to NAO (Fig. 2). The role of ice in the downward intermittency is a bit trickier to assess and is likely a study in its own right. Certainly stratospheric internal variability will contribute to this but also sub-seasonal sea ice variability may enhance/mitigate downward signals. We will include some additional discussion on this topic based on previous studies such as those mentioned by the reviewer.

Please see lines 268-282 and Fig. 5 in the revised manuscript.

4. In my opinion the section “Synoptic linkages and interactions across times scales” is the most novel contribution to the rather large body of literature on this topic and deserves to be highlighted even more. In this context it would be great if the difference between autumn/early and late winter linkages could be discussed in more detail. Which season of sea ice loss is most relevant for the stratospheric pathway, which for the tropospheric pathway. Is it possible to quantify how much of the intermittency is explained by things such as ENSO or synoptic variability? Please also consider discussing/citing this recent paper: E Tyrlis, E Manzini, J Bader, J Ukita, N Hisahi, D Matei, Ural blocking driving extreme Arctic sea-ice loss, cold eurasia and stratospheric vortex weakening in autumn and early winter 2016-2017, Journal of Geophysical Research: Atmospheres 124, 11313-11329

We agree that the synoptic CEN could be expanded to provide more insight into the roles of these processes throughout the cold season. Fig. 7a shows the full synoptic CEN with IR (downward longwave radiation), URALS and ICE, and Fig. 7b shows the CEN-aggregated over six individual months (O, N, D, J, F and M) through the cold season. In general these synoptic linkages show no clear trend evolving from fall to winter but strong variability between individual months. Synoptic linkages with a higher persistence might be seen on longer timescales. For example, an extensive amount of synoptic linkages ↓ICE→↑IR→↑URALS in November and January might help to form the ICE_{Nov}→$URALS_{Dec}$ in the half-monthly (Fig. 2b) and ICE_{Jan}→$URALS_{Feb}$ in monthly CEN (Fig. 2a). Similarly, a large amount of synoptic linkages ↑URALS→↑IR in October and ↑IR→↓ICE in November can reinforce the ICE_{Oct}→$URALS_{Dec}$ linkages in the monthly CEN. This might also explain why the ICE-to-URALS linkage is not found in December as there is only one synoptic linkage ↑URALS→↑IR→↓ICE found in December. The Tyrlis et al. (2019) study about Urals blocking leading to sea ice reduction and subsequent negative NAO conditions via sudden stratospheric warmings is very relevant, and will certainly be brought into the discussion.

As for the El Nino-Southern Oscillation (ENSO), previous work has shown that both ENSO (Figs 5e and 5f in King et al. 2018) and Barents-Kara sea ice (Fig. 5e in King et al. 2016) are associated with the “Scandanivan pattern” mode of variability characterised by high pressure anomalies over the Urals. This suggests that ENSO can potentially interfere with the ICE-NAO stratospheric - for example, in a cold season with low autumn sea ice, an El Niño (La Niña) could reinforce (weaken) the pathway, as discussed in the Discussion section of the submitted manuscript. However, quantitatively, it is tricky to assess the contribution of ENSO to the intermittency with such a short observational record. Moreover, the association between ENSO and the winter NAO/NAM is rather weak (Brönnimann 2007, Domeisen et al., 2019). This can also be seen in Fig. S7 of the submitted manuscript, which shows high (red) and low (blue) Nino3.4 values on both the lower (negative NAO) and upper (positive NAO) sides of the y-axis.

In the revised manuscript, we will expand the discussion of the synoptic linkages and time scale interactions in greater detail, and include a version of Fig. 7b showing the differences between different months. Moreover, we will move Fig. S7 into the main manuscript and expand the discussion as indicated above. In the study we hypothesize that the synoptic variability and ENSO are some possible sources of interference that might lead to intermittency, and show supporting evidence from the CEN. However, we do not provide an in-depth analysis of specific cases of interference, or how the interference occurs. While an interesting investigation in its own right, this is beyond the scope of this paper and is left for future work.

Please see lines 308-328, lines 353-361 and Figs. 7-8 in the revised manuscript.

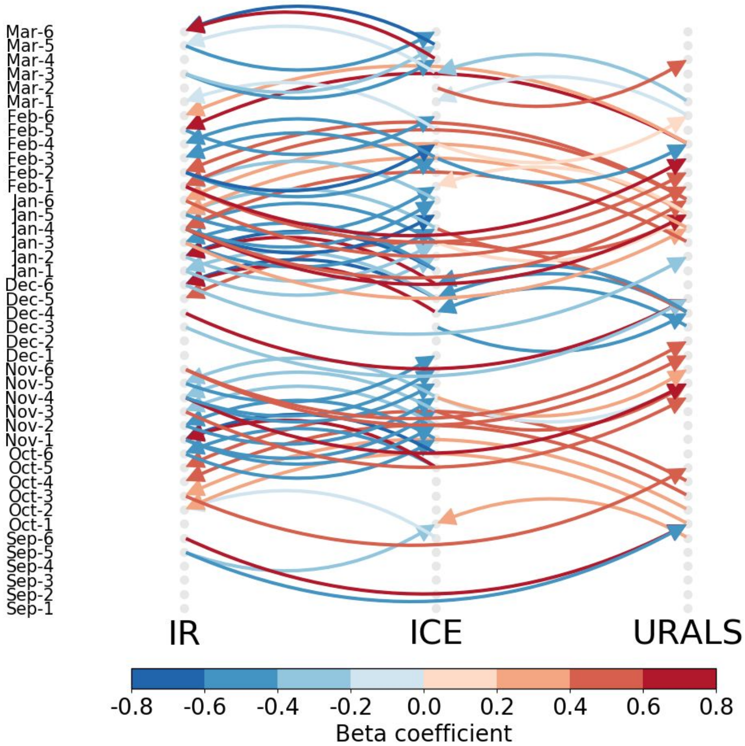

Fig. 7a: As in Fig. S6 in the submitted manuscript, but from the modified CEN algorithm and showing the causal links through the extended ONDJFM cold season (one more month added to the NDJFM cold season used previously).

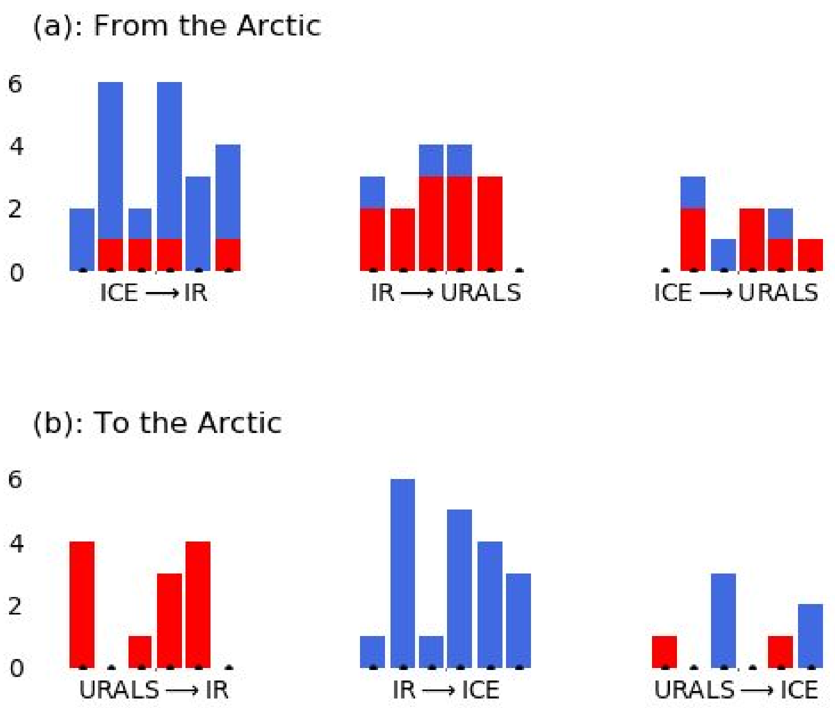

Fig. 7b: As in Fig. 7 in the submitted manuscript, but aggregated by individual months (bars for each linkage are O, N, D, J, F, M from left to right)

5. Technical comments: L3-4: not so obvious to me if really leading to a transition to –NAO (e.g. Karpechko et al 2017)

    It is a good point that the downward coupling following polar vortex weakening is not limited to the European and Atlantic sector. We will mention the AO signature as well.
    Please see line 30.

    L4: The Causal Effect Network. . .

    Thank you, this will be changed.
    Please see line 4.

    L32: Kretschmer et al. 2016 does not use lagged correlations

    The reference will be removed from that sentence.
    Please see line 33.

    L46: do these studies also consider BK sea ice? There is a lot of evidence that sea ice in the Pacific sector leads to a strengthening

    Some of these experiments involved pan-Arctic sea ice reductions instead of Barents-Kara sea ice only. The statement was a general comment alluding to the fact that not all sea ice removal experiments agree with the proposed NAO/AO- response. To be more precise, we will clarify that reduction of sea ice in Pacific can lead to strengthening polar vortex and thus an opposite signed response (Sun et al. 2015).
    Please see lines 49-51.

    L63: Maybe state which linkage you mean exactly.

We refer here to the linkage between sea ice loss and Eurasian cooling. We will state it more clearly.
Please see lines 67-68.

L189: 10,000
Thank you, we will change it.
Please see line 257.

L 203: Why only those where it appears and not all?
Thank you. We think the reviewer was asking why the distributions are composed only of samples in which the linkage appears. The reason is that the beta coefficient can only be calculated when the CEN detects a linkage in a bootstrap sample, so only those samples are included.
Please see line 286-290.

Fig. 3: switching the axes would make it more intuitive.
Thank you for your suggestion. We will play around with switching the axes for the revised manuscript.
Fig. 8 (below) shows the figures where x and y axes are swapped. Things look fine for the monthly and aggregated half-monthly here, but this orientation does not work very well for the unaggregated half-monthly CEN and the pentad CEN (Fig. S2 and S3) since there are many more items on the time axis. In order to keep a consistent format in the manuscript and supplementary documents, we would like to keep the original format of the figure.

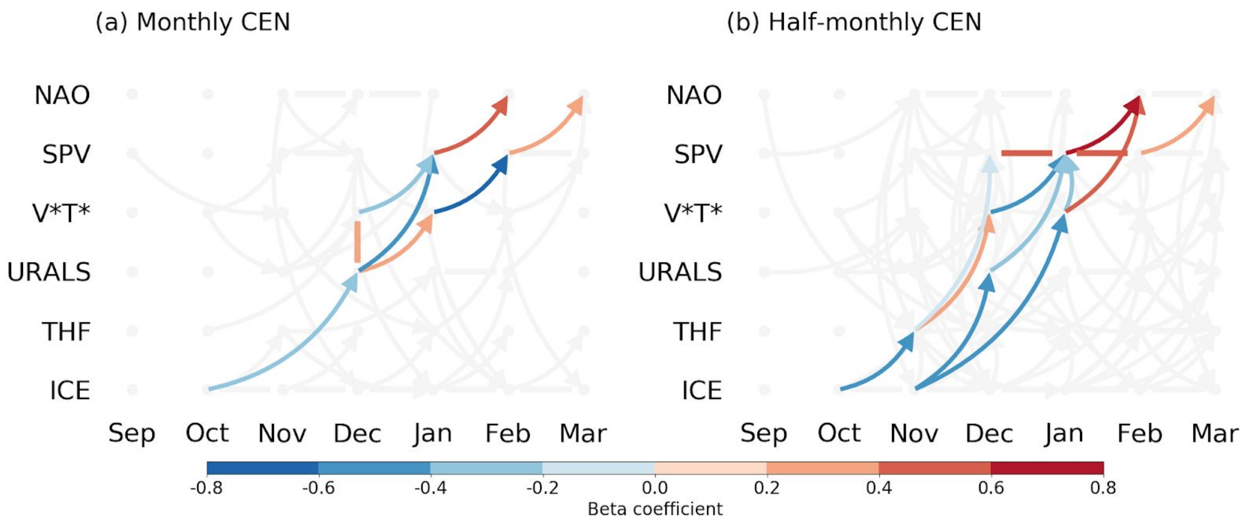

Fig. 8: As in Fig. 3 in the submitted manuscript, but swapping the x and y axes.

L273-277: very interesting thoughts but should rather be moved to discussion
Thank you. We will move this content to the Discussion section.
Please see lines 329-331 and lines 388-389.

References:

Brönnimann, S. "Impact of El Niño–southern oscillation on European climate." *Reviews of Geophysics* 45.3, 2007

Domeisen, D. I., Garfinkel, C. I., and Butler, A. H.: The teleconnection of El Niño Southern Oscillation to the stratosphere, Reviews of Geophysics, 57, 5–47, 2019

King, M. P., Hell, M., and Keenlyside, N.: Investigation of the atmospheric mechanisms related to the autumn sea ice and winter circulation link in the Northern Hemisphere, Climate dynamics, 46, 1185–1195, 2016

King, M. P., Herceg-Bulić, I., Kucharski, F., and Keenlyside, N.:. Interannual tropical Pacific sea surface temperature anomalies teleconnection to Northern Hemisphere atmosphere in November. *Climate dynamics*, *50*(5-6), 1881-1899, 2018

Sun, L., Deser, C., and Tomas, R. A.: Mechanisms of stratospheric and tropospheric circulation response to projected Arctic sea ice loss,Journal of Climate, 28, 7824–7845, 2015

Runge, Jakob, Vladimir Petoukhov, Jonathan F. Donges, Jaroslav Hlinka, Nikola Jajcay, Martin Vejmelka, David Hartman, Norbert Marwan, Milan Paluš, and Jürgen Kurths: “Identifying Causal Gateways and Mediators in Complex Spatio-Temporal Systems.” Nature Communications 6: 8502, 2015

Runge, P. Nowack, M. Kretschmer, S. Flaxman, D. Sejdinovic, Detecting and quan-tifying causal associations in large nonlinear time series datasets. Sci. Adv. 5,eaau4996 (2019)

Saggioro, Elena, and Theodore G. Shepherd. "Quantifying the Timescale and Strength of Southern Hemisphere Intraseasonal Stratosphere-troposphere Coupling." Geophysical Research Letters 46.22, 2019

Intermittency of Arctic-midlatitude teleconnections: stratospheric pathway between autumn sea ice and the winter NAO

Peter Yu Feng Siew[1, 2], Camille Li[1, 2], Stefan Pieter Sobolowski[3, 2], and Martin Peter King[3, 2]

[1]Geophysical Institute, University of Bergen, Bergen, Norway
[2]Bjerknes Centre for Climate Research, Bergen, Norway
[3]NORCE, Bergen, Norway

Correspondence: Peter Yu Feng Siew (yu.siew@uib.no)

Abstract. There is an observed relationship linking Arctic sea ice conditions in autumn to midlatitude weather the following winter. Of interest in this study is a hypothesized stratospheric pathway whereby reduced sea ice in the Barents-Kara Seas enhances upward wave activity and wave-breaking in the stratosphere, leading to a weakening of the polar vortex and a transition of the North Atlantic Oscillation (NAO) to its negative phase. The Causal Effect Networks (CEN) framework is used to explore the stratospheric pathway between late autumn Barents-Kara sea ice and the February NAO, focusing on its seasonal evolution, timescale-dependence, and robustness. Results indicate that the pathway is statistically detectable and has been relatively "active" over the 39-year observational period used here, explaining approximately 26% of the interannual variability in the February NAO. However, a bootstrap-based resampling test reveals that the pathway is highly intermittent: the full stratospheric pathway appears in only 16% of the sample populations derived from observations, with individual causal linkages ranging from 46 to 84% in occurrence rates. The pathway's intermittency is consistent with the weak signal-to-noise ratio of the atmospheric response to Arctic sea ice variability in modelling experiments, and suggests that Arctic-midlatitude teleconnections might be favoured in certain background states. On shorter time scales, the CEN detects two-way interactions between Barents-Kara sea ice and the midlatitude circulation that indicate a role for synoptic variability associated with blocking over the Urals region and moist air intrusions from the Euro-Atlantic sector. This synoptic variability has the potential to interfere with the stratospheric pathway, thereby contributing to its intermittency. This study helps quantify the robustness of causal linkages within the stratospheric pathway, and provides insight into which linkages are most subject to sampling issues within the relatively short observational record. Overall, the results should help guide the analysis and design of ensemble modelling experiments required to improve physical understanding of Arctic-midlatitude teleconnections.

1 Introduction

Autumn sea ice is a potential source of skill in predicting the winter North Atlantic Oscillation (NAO), and hence, European climate (Scaife et al., 2014; Wang et al., 2017; Hall et al., 2017). One proposed mechanism for the relationship focuses on the Barents-Kara Seas, a region with seasonal ice cover that has exhibited strong negative trends during the cold season over the last decades (Cavalieri and Parkinson, 2012; Serreze and Stroeve, 2015; Onarheim and Årthun, 2017). According to this mechanism, reduced Barents-Kara sea ice triggers a wave response that constructively interferes with the climatological stationary wave pattern (Peings and Magnusdottir, 2014; Kim et al., 2014; Sun et al., 2015; Nakamura et al., 2016; Wu and Smith, 2016; Hoshi et al., 2017; Zhang et al., 2018a; De and Wu, 2018), enhancing upward propagation of planetary waves that weakens the stratospheric polar vortex (Nishii et al., 2009; Garfinkel et al., 2010; Smith et al., 2010). Downward coupling from the stratosphere to the troposphere subsequently produces circulation anomalies that resemble the negative phase of the NAO or Arctic Oscillation (AO) (Baldwin and Dunkerton, 1999; Polvani and Waugh, 2004), along with its attendant climate effects (Hurrell, 1995).

A delayed stratospheric pathway linking sea ice and the NAO is suggested by observations, but its exact nature is somewhat unclear. The observational evidence (e.g., García-Serrano et al., 2015; King et al., 2016; Koenigk et al., 2016) hinges on lagged correlations such as the one shown in Fig. 1a (similar to Fig. 10c in García-Serrano et al. (2015) and Fig. 6b in King et al. (2016)): less Barents-Kara sea ice in November is associated with higher polar cap heights in the stratosphere (i.e., polar vortex weakening), and a subsequent downward propagation of the height anomalies into the troposphere through the winter season, consistent with the appearance of negative NAO conditions several months later. However, the stationarity and statistical significance of this signal has been questioned when using longer records that extend back before the satellite era (Hopsch et al., 2012; Kolstad and Screen, 2019). In fact, the strength and timing of the signal can change when the observational period in Fig. 1a is extended by just several additional winters, showing a statistically insignificant autumn sea ice connection to the winter NAO via the stratosphere (Fig. 1b).

Evidence from modelling experiments is even more difficult to interpret because the relationship between Barents-Kara sea ice and the NAO is not robust in simulations. Some studies find a clear stratospheric signal after removing sea ice, leading to a weakening of the polar vortex and a negative NAO (Kim et al., 2014; Nakamura et al., 2015; Sun et al., 2015). A negative NAO response to sea ice loss is also possible, although much weaker, if the stratospheric pathway is not well represented or artificially suppressed (Liptak and Strong, 2014; Sun et al., 2015; Wu and Smith, 2016; Nakamura et al., 2016; Zhang et al., 2018a; De and Wu, 2018). However, other modelling studies show a weak or even positive NAO response when sea ice is reduced (Singarayer et al., 2006; Strey et al., 2010; Orsolini et al., 2012; Cassano et al., 2014; Screen et al., 2014), and we lack a comprehensive understanding of why model results are so different (Screen et al., 2018). One reason may be that the atmospheric response depends on where and when sea ice is removed; for example, some studies have shown that sea ice loss in the Pacific sector leads to a strengthening of the polar vortex (Sun et al., 2015; Screen, 2017; McKenna et al., 2018), and that winter ice loss may be more influential than autumn ice loss in weakening and shifting the jet stream (Blackport and Screen, 2019). Other possible reasons include nonlinearities with respect to the amplitude of sea ice loss (Petoukhov and Semenov, 2010; Semenov and Latif, 2015; Chen et al., 2016; Overland et al., 2016), and dependence of the atmospheric response on the background state (Smith et al., 2017, 2019; Labe et al., 2019).

Overall, isolating the sea ice influence on the midlatitudes remains a challenge in part because it is a search for causal drivers in a tightly coupled system with large internal variability (Shepherd, 2016). This internal atmospheric varibility itself has well-known effects on Arctic climate over a range of time scales. Synoptic weather systems carry heat and moisture poleward from the North Atlantic, and are associated with moist intrusions that have been shown to warm the Arctic and melt sea ice (Woods et al., 2013; Park et al., 2015a, b; Gong and Luo, 2017; Kim et al., 2017; Lee et al., 2017). Feedbacks between sea ice and the NAO acting on intraseasonal time scales can yield oppsite-signed relationships depending on the time lag considered: anomalously low Barents-Kara sea ice concentrations are favoured by positive NAO conditions (Fang and Wallace, 1994; Deser et al., 2000), but are also part of an ice perturbation pattern that has been found to produce negative NAO conditions (Magnusdottir et al., 2004; Deser et al., 2004; Kvamstø et al., 2004; Strong et al., 2009; Deser et al., 2010; Wu and Zhang, 2010). The causality problem with respect to sea ice extends beyond the NAO to other midlatitude phenomena such as Eurasian cooling, for which one finds numerous studies arguing both for (Outten and Esau, 2012; Mori et al., 2014, 2019) and against (McCusker et al., 2016; Sorokina et al., 2016; Ogawa et al., 2018; Blackport et al., 2019) sea ice loss being responsible for the recent spate of extreme winters.

In the present study, we revisit the observed relationship between autumn Barents-Kara sea ice and the winter NAO with the goal of quantifying the robustness of the stratospheric linkage. In other words, we ask how systematically the stratospheric linkage has appeared during the satellite period. While sampling issues are unavoidable when using a short observational record with large internal variability, our analysis attempts to account for this by exploring the idea that weak but statistically significant signals may arise from a teleconnection pathway that is only intermittently active.

We begin with a description of data and methods (section 2), including a Causal Effect Networks (CEN) approach that provides a statistical framework for assessing causality (applied to climate problems by studies such as Ebert-Uphoff and Deng, 2012; Runge et al., 2014; Kretschmer et al., 2016, 2018). Results showing that the pathway is indeed detectable but exhibits a high level of intermittency are presented in section 3, and the implications for understanding present day Arctic-midlatitude teleconnections are discussed in section 4. We end with some concluding remarks in section 5.

2 Data and Methods

2.1 Reanalysis data

The Causal Effect Networks (CEN) approach requires indices (time series) of variables representing key processes in the dynamical mechanism being studied. In our study, we use sea ice area fraction, surface sensible heat flux, surface latent heat flux, sea level pressure, meridional wind, temperature, geopotential height, and downard thermal radiation at the surface. Raw daily data for the period 1979 to 2018 are from the European Center for Medium-Range Weather Forecasts (ECMWF) ERA-Interim reanalysis (Dee et al., 2011). The seasonal cycle is removed at each grid point by subtracting the climatological daily mean to obtain anomalies of each variable, and the data are detrended. The trend is removed through all the days of the year (1 January, 2 January, etc.). The following indices are then calculated from the reanalysis data from September to March:

- Barents-Kara sea ice (ICE): sea ice area fraction averaged over 70°-80° N, 30°-105° E (Fig. 2a)

– Barents-Kara turbulent heat flux (THF): sum of surface sensible and latent heat flux averaged over 70°-80° N, 30°-105° E (Fig. 2b), with positive defined as heat flux from the ocean to the atmosphere

– stratospheric polar vortex strength (SPV): negative of geopotential height poleward of 60° N (Fig. 2c) averaged between 10-100 hPa, as defined by Kretschmer et al. (2016), such that positive values of the index indicate a stronger polar vortex

– Urals sea level pressure (URALS): sea level pressure averaged over 45°-70° N, 40°-85° E (Fig. 2d)

– downward longwave radiation (IR): downward thermal radiation at the surface averaged over 70°-90° N (Fig. 2e)

– poleward eddy heat flux (V*T*): product of V* and T* at 100 hPa averaged over 45°-75° N (Fig. 2f), where V and T denote the meridional wind velocity and air temperature respectively, and the superscript * indicates deviations from the zonal mean

– North Atlantic Oscillation index (NAO): from the Climate Prediction Center, based on Rotated Principal Component Analysis of 500 hPa geopotential height, see details at https://www.cpc.ncep.noaa.gov/products/precip/CWlink/pna/nao.shtml

Finally, the daily indices are averaged up to monthly, half-monthly and pentad means for the different analyses carried out in this study.

2.2 Causal Effect Networks (CEN)

The CEN algorithm is a causal inference framework (Runge et al., 2014, 2019) aimed at identifying causal relationships between variables of interest. It was previously used to study Arctic-midlatitude teleconnections by Kretschmer et al. (2016, 2018). Essentially, given a set of indices such as the ones described above, a CEN is constructed following three steps: 1) identify potential causal drivers of each index (condition selection), 2) identify the true causal drivers using these potential causal drivers as a “conditioning set”, and 3) quantify the strength of the causal relationship. We will illustrate the algorithm using January stratospheric polar vortex strength (SPV_{Jan}) as an example. Readers are refered to Kretschmer et al. (2016) and Runge et al. (2019) for a full description of the CEN algorithm.

In the first step, we find all possible drivers for SPV_{Jan}. A preliminary list of drivers is generated by calculating the Pearson correlation r between SPV_{Jan} and all other indices (including SPV itself) in the preceding months, up to a maximum lag of 2 months (i.e., November and December for this example). Indices with significant correlations are retained, where an optimal significance level is determined using the Akaike information criterion (AIC). The AIC results in the selection of a 20% significance level for the case of SPV_{Jan} (note that the AIC allows for these rather liberal significance levels in the first step, but more stringent levels are used later in the second step). This leaves us with the following possible drivers: $V^*T^*_{Dec}$, $URALS_{Dec}$, SPV_{Dec} and $URALS_{Nov}$. This list is sorted in descending order according to the absolute value of the Pearson correlation coefficient. Next, we test for the conditional independence of all four possible drivers with SPV_{Jan} by calculating partial correlations, controlling for the effect of each driver one at a time starting from the top of the sorted list. If a driver passes the partial correlation test, it is retained in the list of possible drivers; if it does not pass, it is removed from the list, meaning it is no longer in the conditioning set. For example, the partial correlation between $\mathrm{URALS_{Nov}}$ and $\mathrm{SPV_{Jan}}$ controlling for $\mathrm{V^*T^*_{Dec}}$ is, following the notation of Kretschmer et al. (2016):

$$\rho(\mathrm{URALS_{Nov}},\, \mathrm{SPV_{Jan}} \mid \mathrm{V^*T^*_{Dec}}) = -0.274, \tag{1}$$

where

$$\rho(x,\, y \mid z) = \frac{r_{xy} - r_{xz} r_{yz}}{\sqrt{1 - r_{xz}^2}\,\sqrt{1 - r_{yz}^2}} \tag{2}$$

The partial correlation is significant at the 20% level (p-value = 0.105), therefore, $\mathrm{URALS_{Nov}}$ is retained as a possible driver of $\mathrm{SPV_{Jan}}$. After going through the entire list, $\mathrm{SPV_{Dec}}$ is eliminated, leaving us with three possible drivers of $\mathrm{SPV_{Jan}}$: $\mathrm{URALS_{Nov}}$, $\mathrm{URALS_{Dec}}$ and $\mathrm{V^*T^*_{Dec}}$.

In the second step, we retest all possible links (for all indices in the preceding two months, including those rejected in the first step) with $\mathrm{SPV_{Jan}}$, controlling for the *combined effect* of the possible drivers (conditioning set) identified in the first step. This step helps account for false positives when working with highly interdependent time series (as is often the case with climate indices), and enhances detection power (Runge et al., 2019). Specifically, the test for $\mathrm{SPV_{Jan}}$ is:

$$\rho(\mathrm{X},\, \mathrm{SPV_{Jan}} \mid \mathrm{URALS_{Nov}},\, \mathrm{URALS_{Dec}},\, \mathrm{V^*T^*_{Dec}}), \tag{3}$$

where X represents all indices of ICE, THF, URALS, V*T*, SPV and NAO in both November and December. Any X producing a significant partial correlation in Eq. 3 is regarded as a causal driver of $\mathrm{SPV_{Jan}}$. The conditioning set excludes X when X is being tested, for example:

$$\rho(\mathrm{V^*T^*_{Dec}},\, \mathrm{SPV_{Jan}} \mid \mathrm{URALS_{Nov}},\, \mathrm{URALS_{Dec}}) = -0.453 \tag{4}$$

which is significant at the 5% level (p-value=0.00629). Testing all X leaves us with three causal drivers of $\mathrm{SPV_{Jan}}$: $\mathrm{URALS_{Nov}}$, $\mathrm{URALS_{Dec}}$ and $\mathrm{V^*T^*_{Dec}}$. Note that these are the same causal drivers identified in the first step, meaning that no new drivers are reintroduced in the second step in this case. As an additional refinement, the Hochberg-Benjamini false discovery rate (FDR) control may be used to account for the multiple testing problem (Kretschmer et al., 2018; Runge et al., 2019).

In the third step, we use a multiple regression equation to quantify the influence of causal drivers and simultaneous influences on $\mathrm{SPV_{Jan}}$:

$$\mathrm{SPV}^s_{\mathrm{Jan}} = \beta_0 + \beta_1 * \mathrm{URALS}^s_{\mathrm{Nov}} + \beta_2 * \mathrm{URALS}^s_{\mathrm{Dec}} + \beta_3 * \mathrm{V^*T^*}^s_{\mathrm{Dec}} + \beta_4 * \mathrm{Y}^s_{\mathrm{Jan}} \tag{5}$$

where the β values are regression coefficients for the standardized regressors $\mathrm{URALS}^s_{\mathrm{Nov}}$, $\mathrm{URALS}^s_{\mathrm{Dec}}$, $\mathrm{V^*T^*}^s_{\mathrm{Dec}}$, $\mathrm{Y}^s_{\mathrm{Jan}}$, and the superscript s indicates a standardized index. The inclusion of Y allows us to check for significant simultaneous relationships between all indices. By standardizing, the interpretation is that changing a certain regressor by one standard deviation changes $\mathrm{SPV_{Jan}}$ by β standard deviations, provided that all other variables are held fixed.

A two-tailed t-test is used for significance testing. For the AIC in step one, a significance set of (5%, 10%, 20%) is used. There are no substantial changes to the main messages when using other significance sets (Fig. S4). A significance level of 5% is used in the second and third steps.

The above example illustrates how the CEN algorithm identifies and evaluates causal drivers of SPV_{Jan}. In order to construct the complete monthly and half-monthly CENs, we identify causal drivers for all our chosen indices (ICE, THF, URALS, V*T*, SPV and NAO) during the extended winter season (NDJFM). September to December (January to March) indices are taken over the period of 1979 to 2017 (1980 to 2018). All Pearson correlations and partial correlations (first and second steps) and the multiple regressions (third step) are thus based on indices with a sample size of 39 winter seasons. A similar procedure is used for the pentad CEN, but with a maximum lag of two pentads to capture processes occurring on synoptic time scales.

3 Results

This section describes results from our exploration of the ICE-NAO stratospheric pathway using the CEN framework (section 3.1), including an assessment of its strength (section 3.2) and intermittency (section 3.3) in the observational record. We also explore processes occurring on shorter timescales, and discuss how these effects may reinforce or interrupt the stratospheric pathway (section 3.4).

3.1 Seasonally evolving ICE-NAO pathway

We begin by examining pathways from Barents-Kara sea ice to the NAO proposed by previous studies. The CEN analysis follows the approach of Kretschmer et al. (2016), but keeps individual months separate rather than considering the DJF period as a whole. This allows us to capture the seasonal evolution of pathways through the cold season.

The CEN (Fig. 3) shows evidence for a stratospheric pathway leading from autumn sea ice perturbations in the Barents-Kara Seas to a late winter NAO response. This pathway appears using both monthly (Fig. 3a) and half-monthly (Fig. 3b) averages as input to the CEN, albeit with slight differences in timing. The half-monthly CEN in Fig. 3b is displayed such that individual half-monthly linkages (shown in Fig. S2) are aggregated into full months to allow for direct comparison to Fig. 3a.

Coloured arrows in the network diagrams highlight the ICE-NAO stratospheric pathway, where red indicates positive relationships and blue indicates negative relationships (the exact values correspond to the beta coefficients in the multiple regression equation, e.g., Eq. 5). Grey arrows show other linkages that are statistically significant, including some tropospheric pathways that also contribute to the ICE-NAO relationship. A figure including all the identified causal linkages and autocorrelations appears in the supplementary material (Fig. S1). For the monthly CEN, the stratospheric pathway is

$$\downarrow ICE_{Oct} \Rightarrow \uparrow URALS_{Dec} \Rightarrow \uparrow V^{*}T^{*}_{Dec/Jan} \Rightarrow \downarrow SPV_{Jan/Feb} \Rightarrow \downarrow NAO_{Feb/Mar}$$

where we use the notation A $\Rightarrow$ B to indicate index A as a "driver" of index B, and $\downarrow$ and $\uparrow$ to represent a decrease or increase, respectively, of the indices. The pathway is described for the case of a negative sea ice perturbation leading to a negative NAO.

For the half-monthly CEN, the pathway may be summarized as:

$\downarrow \mathrm{ICE}_{\mathrm{Oct/Nov}} \Rightarrow \uparrow \mathrm{THF}_{\mathrm{Nov}} \Rightarrow \uparrow \mathrm{URALS}_{\mathrm{Dec}} \Rightarrow \uparrow \mathrm{V^*T^*}_{\mathrm{Dec/Jan}} \Rightarrow \downarrow \mathrm{SPV}_{\mathrm{Dec/Jan/Feb}} \Rightarrow \downarrow \mathrm{NAO}_{\mathrm{Feb/Mar}}$

Using the finer half-monthly resolution in the CEN prevents shorter timescale processes (such as linkages through THF) from being averaged out.

The CEN results illustrate how the stratospheric pathway unfolds through the winter season. The timing is in general agreement with previous observational studies, suggesting that the involvement of the stratosphere introduces a few months' delay in the NAO response to Barents-Kara sea ice variability (Kim et al., 2014; García-Serrano et al., 2015; Jaiser et al., 2016; King et al., 2016; Kretschmer et al., 2016; Yang et al., 2016). The causal linkages are consistent with the idea that Arctic sea ice reduction enhances upward wave activity through constructive interference between forced Rossby waves and the climatological stationary waves (Garfinkel et al., 2010; Smith et al., 2010). The resulting increase in wave-breaking in the stratosphere decelerates the polar vortex (Charney and Drazin, 1961), which in turn leads to tropospheric circulation anomalies and surface impacts via downward coupling (Baldwin and Dunkerton, 1999). Some features of the pathway, such as the relatively long lagged relationship of autumn sea ice to December Urals sea level pressure, are not well understood, an issue that will be further discussed in section 4.

We will focus on the stratospheric pathway from $\mathrm{ICE}_{\mathrm{Oct}}$ to $\mathrm{NAO}_{\mathrm{Feb}}$ in the monthly CEN, as this timing yields the strongest negative ICE-NAO correlation (Fig. S5). The correlation between $\mathrm{ICE}_{\mathrm{Nov}}$ and $\mathrm{NAO}_{\mathrm{Jan}}$ is equally strong, but the causal pathway goes through the troposphere only (Fig. S1b) and is not a focus of this study. Results from the half-monthly CEN yield consistent messages, and will be brought into the discussion where relevant.

3.2 Strength of the pathway

An interesting question is how to assess the strength of the ICE-NAO stratospheric pathway as a whole, and what insights may be gained by such an assessment.

The CEN analysis yields a set of beta coefficients (colours of the arrows in Fig. 3) that describe the strength of individual causal linkages in our network. Following Runge et al. (2015), the *total causal effect* of the stratospheric pathway from $\mathrm{ICE}_{\mathrm{Oct}}$ to $\mathrm{NAO}_{\mathrm{Feb}}$ may be calculated by summing over the product of beta coefficients along the two relevant chains of linkages from Fig. 3a:

$$\downarrow \mathrm{ICE}_{\mathrm{Oct}} \xRightarrow{-0.326} \uparrow \mathrm{URALS}_{\mathrm{Dec}} \xRightarrow{0.390} \uparrow \mathrm{V^*T^*}_{\mathrm{Dec}} \xRightarrow{-0.368} \downarrow \mathrm{SPV}_{\mathrm{Jan}} \xRightarrow{0.426} \downarrow \mathrm{NAO}_{\mathrm{Feb}}\ (0.0199)$$

205

$$\downarrow \mathrm{ICE}_{\mathrm{Oct}} \xRightarrow{-0.326} \uparrow \mathrm{URALS}_{\mathrm{Dec}} \xRightarrow{-0.449} \downarrow \mathrm{SPV}_{\mathrm{Jan}} \xRightarrow{0.426} \downarrow \mathrm{NAO}_{\mathrm{Feb}}\ (0.0624)$$

The total causal effect (0.0199 + 0.0624 = 0.0823) tells us that a one-standard deviation perturbation in $\mathrm{ICE}_{\mathrm{Oct}}$ yields a like-signed response of 8% of one-standard deviation in February NAO (Runge et al., 2015).

A comparison between the stratospheric and tropospheric ICE-NAO pathways shows that the latter are generally stronger in the CEN framework. Table 1 summarizes the causal effect of the three full pathways (Fig. S6). Our main stratospheric pathway of interest from $\mathrm{ICE}_{\mathrm{Oct}}$ to $\mathrm{NAO}_{\mathrm{Feb}}$ is comparable in strength to the pathway from $\mathrm{ICE}_{\mathrm{Oct}}$ to $\mathrm{NAO}_{\mathrm{Mar}}$ (0.0823 and

0.0872). The latter has both stratospheric and tropospheric chains, accounting for 30% (0.0258/(0.0614+0.0258)) and 70% (0.0614/(0.0614+0.0258)) of the total causal effect, respectively. The $\downarrow$ $\mathrm{ICE_{Jan}} \Rightarrow\downarrow \mathrm{NAO_{Mar}}$ tropospheric pathway is the strongest in terms of the total causal effect (0.137), primarily because it involves fewer linkages. Overall, the larger causal effect of the tropospheric pathways is perhaps unsurprising, given that the stratospheric pathway may be disrupted by internal variability (noise) from both the troposphere and the stratosphere.

An alternative view of the pathway strength comes from considering the amount of February NAO variance explained by the various linkages along the pathway using a multiple linear regression framework. This gives a sense of the relative importance of each linkage, and how information passes through the pathway. The full pathway can be represented by the following regression equation:

$$\mathrm{NAO_{Feb}} = \kappa_0 + \kappa_1 \cdot \mathrm{ICE_{Oct}} + \kappa_2 \cdot \mathrm{URALS_{Dec}} + \kappa_3 \cdot \mathrm{V^*T^*_{Dec}} + \kappa_4 \cdot \mathrm{SPV_{Jan}} \tag{6}$$

where κ_0 is a constant and κ_1, κ_2, κ_3, κ_4 are the regression coefficients for the standardized regressors $\mathrm{ICE_{Oct}}$, $\mathrm{URALS_{Dec}}$, $\mathrm{V^*T^*_{Dec}}$ and $\mathrm{SPV_{Jan}}$, respectively. The importance of the regressors may be quantified in different ways, for example:

a) cumulative $\mathrm{NAO_{Feb}}$ variance explained as regressors are included, calculated by successively adding terms in Eq. 6 from left to right (orange bars in Fig. 4), e.g. for $\mathrm{V^*T^*_{Dec}}$:

$$\mathrm{NAO_{Feb}} = \kappa_0^a + \kappa_1^a \cdot \mathrm{ICE_{Oct}} + \kappa_2^a \cdot \mathrm{URALS_{Dec}} + \kappa_3^a \cdot \mathrm{V^*T^*_{Dec}} \tag{7}$$

b) $\mathrm{NAO_{Feb}}$ variance explained by individual regressors, calculated via a simple bivariate regression between each regressor and $\mathrm{NAO_{Feb}}$ (blue bars), e.g., for $\mathrm{V^*T^*_{Dec}}$:

$$\mathrm{NAO_{Feb}} = \kappa_0^b + \kappa_3^b \cdot \mathrm{V^*T^*_{Dec}} \tag{8}$$

c) reduction in $\mathrm{NAO_{Feb}}$ variance explained when individual regressors are removed, calculated by removing the term from the regression equation (green bars), e.g., for $\mathrm{V^*T^*_{Dec}}$:

$$\mathrm{NAO_{Feb}} = \kappa_0^c + \kappa_1^c \cdot \mathrm{ICE_{Oct}} + \kappa_2^c \cdot \mathrm{URALS_{Dec}} + \kappa_4^c \cdot \mathrm{SPV_{Jan}} \tag{9}$$

Both the blue and green bars in Fig. 4 provide a measure of the contribution of individual regressors, while comparison of these with the orange bars gives some indication of whether information from a given regressor is redundant.

The stratospheric pathway explains 26% of the variance in the February NAO (Fig. 4). The cumulative variance explained (orange bars) increases from 11% to 26% as regressors are added (moving from left to right), indicating that each linkage in the pathway adds some useful information. This result is consistent with other estimates from observations, but likely represents an upper limit as the Barents-Kara sea ice and NAO relationship is shown to be particularly strong during the current reanalysis period compared to the rest of the twentieth century (Kolstad and Screen, 2019).

While successive linkages in the pathway add explanatory power, they are not independent. Comparing the orange and blue bars, we see that the increase of cumulative explained variance moving from left to right is much less than the explained variance from each individual regressor. For example, while SPV_{Jan} explains the most NAO variance of any individual regressor (18%), its removal from the full regression does not have much effect (3% reduction in explained variance), However, we know that variability in upward wave activity and variability in the polar vortex are closely related, so in a sense, it is not physically meaningful to consider one in isolation of the other. Removing both $V^*T^*_{Dec}$ and SPV_{Jan} from the regression equation results in a 8% reduction (not shown) in explained variance, which is perhaps a more representative estimate of the stratosphere's contribution. Sea ice appears to impart information that cannot be explained by the other three regressors (6% reduction in explained NAO variance when removed), but this may also be a result of atmosphere-ice feedbacks explored in section 3.4.

Overall, these analyses show a role for the stratosphere in connecting autumn ICE to late winter NAO, but one that accounts for a modest fraction of the total NAO variance. In the next section, we will further explore reasons for this relatively weak ICE-NAO covariability.

3.3 Intermittency of the pathway

The ICE-NAO stratospheric pathway identified by the CEN comprises statistical relationships inferred from a relatively short observational record of only 39 winters. It is meaningful to ask how robust the pathway is, that is, how systematically the relevant statistical relationships occur in the record. To assess the robustness, we perform a bootstrapping test, where bootstrap samples are created by randomly selecting 39 winters with replacement from the entire reanalysis period. The CEN of each sample is then constructed. This procedure is repeated 10,000 times.

The bootstrapping results (Fig. 5) indicate that the stratospheric pathway is intermittent. Percentages show the occurrence rate of individual segments in the pathway within the bootstrap sample population (see Fig. S7 for occurrence rates of other statistically significant linkages). By this measure, it is clear that individual segments have varying levels of intermittency, ranging from 46% for the segment $\downarrow SPV_{Jan} \Rightarrow \downarrow NAO_{Feb}$ to 84% for the segment $\uparrow V^*T^*_{Dec} \Rightarrow \downarrow SPV_{Jan}$. The full stratospheric pathway (the sequence of all four segments) is detected in only 16% of the samples, suggesting that it does not occur systematically during every winter season. An alternative three-segment pathway $\downarrow ICE_{Oct} \Rightarrow \uparrow URALS_{Dec} \Rightarrow \downarrow SPV_{Jan} \Rightarrow \downarrow NAO_{Feb}$ is slightly less intermittent (22% occurrence rate), but its physical interpretation is unclear given that there is no linkage through V*T* to the polar vortex. These intermittency results are a likely reason why detection of the pathway is sensitive to the choice of observational period (Fig. 1), and suggests that it may be favoured in certain background states (Overland et al., 2016; Smith et al., 2017).

The existence of intermittency in the stratospheric pathway is consistent with previous suggestions that internal variability modulates the influence of Arctic sea ice on the midlatitude circulation (Screen et al., 2014; Overland et al., 2016; Shepherd, 2016). An examination of where in the pathway the intermittency is strongest provides clues to its origins. For example, the upward coupling from sea ice to the stratosphere includes the segments $\downarrow ICE_{Oct} \Rightarrow \uparrow URALS_{Dec}$ and $\uparrow URALS_{Dec} \Rightarrow \uparrow V^*T^*_{Dec}$, whose occurrence rates are 50% and 74%, respectively. The occurrence of these two linkages together is seen in about 41% out of 10,000 bootstrap samples, meaning that most of the time when the $\downarrow ICE_{Oct} \Rightarrow \uparrow URALS_{Dec}$ linkage is detected, the subsequent linkage to $V^*T^*_{Dec}$ follows. Conversely, when the $\uparrow URALS_{Dec} \Rightarrow \uparrow V^*T^*_{Dec}$ linkage is detected, it is preceded by the $\downarrow ICE_{Oct} \Rightarrow \uparrow URALS_{Dec}$ linkage in only about half the cases. An obvious source of the intermittency in both segments (individually and in terms of their "combined" occurrence rate) is regional SLP variability over the Urals related to atmospheric internal variability. Similarly, the downward coupling from SPV to NAO is vulnerable to both stratospheric and tropospheric internal variability, leading to a relatively low occurrence rate of 46%. This is consistent with the idea that not all polar vortex weakening events affect the tropospheric circulation (Karpechko et al., 2017). Most robust is the $\uparrow V^*T^*_{Dec} \Rightarrow \downarrow SPV_{Jan}$ linkage (84%), which arises from well-known physical processes related to upward planetary wave flux and polar vortex weakening. Sea ice variability can also contribute to intermittency in the pathway through higher frequency synoptic processes, a topic we will explore in section 3.4.

The strength of the segments in the pathway also exhibits large variability among the bootstrap samples. This can be seen in histograms of the beta coefficients for all segments in the pathway (Fig. 5). While the beta coefficients exhibit ranges of up to 0.5 for any given segment, the sign is always the same, indicating that the sign of the relationship between variables is robust. The observed beta coefficients (black lines) for the reanalysis period itself fall within the spread of the distributions. Note that the distributions are composed only of samples in which the linkage of interest is detected by the CEN algorithm (i.e., a beta coefficient can be calculated from Eq. 5), which is why some of the distributions appear skewed. This is particularly true for the linkages that are least robust (the first and last segments, for which the observed beta coefficients are towards the weaker end of the distributions). Overall, these results indicate that even when the stratospheric pathway is active, there is substantial interannual variability in how it manifests.

3.4 Synoptic linkages and interactions across times scales

In the monthly CEN analysis, there are simultaneous relationships between Barents-Kara sea ice, Urals sea level pressure and the NAO (Fig. 6) that point to linkages through shorter timescale synoptic processes. For example, the NAO shows significant negative simultaneous relationships with Barents-Kara sea ice (positive NAO with reduced ice) in December and March, reflecting a well-known pattern of atmospheric forcing on sea ice via anomalies in surface heat fluxes driven by wind and temperature variability (Fang and Wallace, 1994; Deser et al., 2000). Additional simultaneous relationships between sea ice, turbulent heat flux, and Urals sea level pressure are consistent with synoptic features related to cyclones (Boisvert et al., 2016; Wickström et al., 2019) and moist intrusions (Woods et al., 2013; Park et al., 2015b) entering the Arctic. Moist intrusions in particular appear to occur preferentially during the positive phase of the NAO (Luo et al., 2017) and have been shown to lead to enhanced downward longwave radiation, surface warming, and sea ice reductions (Gong and Luo, 2017; Chen et al., 2018). We explore the possible influences of such events within the CEN framework by using higher frequency data to capture the relevant synoptic processes. The input data are pentad (5-day) means of Barents-Kara sea ice (ICE), Urals sea level pressure (URALS) and downward longwave radiation (IR). The maximum lag is set to two pentads (10 days) to isolate the synoptic timescale. The results are summarized in Fig. 7 by summing the number of times a linkage appears in each month from Fig. S8. The maximum count for a given linkage in a month is 12 (six pentads in a month and up to 2-pentad lag considered). Autocorrelation is strong on these short time scales, and thus is not used to reject causal linkages in the partial correlation tests.

The CEN detects synoptic-scale influences from the Arctic to the midlatitudes that reinforce linkages found in the monthly analysis. A linkage from ICE to URALS appears regularly throughout the winter season (Fig. 7a), both indirectly through

IR and as a direct connection, and in the correct sense to contribute to the $\downarrow \mathrm{ICE}_{\mathrm{Oct/Nov}} \Rightarrow \uparrow \mathrm{URALS}_{\mathrm{Dec}}$ linkage shown in the monthly and half-monthly CENs (Fig. 3). The $\downarrow$ ICE $\Rightarrow \uparrow$ IR linkage (blue bars, first histogram in Fig. 7a) follows from the idea that sea ice retreat exposes open ocean, which is a local evaporative source for water vapour, leading to a moister, optically thicker atmosphere (Kim and Kim, 2017; Zhong et al., 2018). The linkage $\uparrow$ IR $\Rightarrow \uparrow$ URALS (red bars, second histogram in Fig. 7a) is consistent with a suggested mechanism whereby the resulting surface warming weakens zonal wind locally and promotes blocking over the Urals (Luo et al., 2016). These synoptic processes, if habitually occurring, can imprint onto longer timescales, but may also produce interference effects, as seen by the appearance of opposite-signed causal relationships from those described above from time to time through the winter season.

At the same time, causal effects from the midlatitudes to the Arctic are also detected, consistent with an influence from moisture transport by cyclones or synoptic moist intrusions (Fig. 7b). This is represented by the $\uparrow$ URALS $\Rightarrow \uparrow$ IR linkage (most frequently observed in October, January and February) and the $\uparrow$ IR $\Rightarrow \downarrow$ ICE linkage (most frequently observed in November, January and February), which reflect the transport of moist air into the dry Arctic atmosphere by the large-scale flow or by cyclones tracking into the Barents. These midlatitude-to-Arctic linkages have a uniform sign (all red bars in first histogram, all blue bars in second histogram), suggesting that the effect of the relevant processes is rather systematic despite exhibiting month-to-month variability. We also detect a direct linkage from the Urals to Barents-Kara sea ice that can be of either sign. In the slightly more frequent negative sense ($\uparrow$ URALS $\Rightarrow \downarrow$ ICE), it can be interpreted as a direct effect of warm air advection and mechanical forcing of the ice cover from enhanced southerlies over the Barents-Kara region (Sorokina et al., 2016; McCusker et al., 2016). Together, these synoptic linkages show how Urals SLP variability, which has a large internally generated component, can reinforce or interrupt the ICE-NAO stratospheric pathway.

Given that our understanding of Arctic-midlatitude teleconnections must account for the combined influences of such linkages across regions and time scales, it is no surprise that we have yet to identify a definitive set of mechanisms. Implications of such scale interactions and how they relate to viewpoints presented in previous studies are further discussed in section 4.

4 Discussion

This study quantifies the robustness of atmospheric teleconnections between the Arctic and midlatitudes, documenting their high level of intermittency in the observational record. In a bootstrapping test, the full stratospheric pathway emerges in only 16% of the sample populations derived from the observations (Fig. 5). The existence of intermittency is likely why studies using various analytical approaches and time periods find teleconnections that differ in pattern, timing, robustness and apparent mechanisms (Overland et al., 2016; Francis, 2017; Cohen et al., 2018; Overland and Wang, 2018; Cohen et al., 2019). In this section we discuss some of the factors that may contribute to the intermittency. Of course, anything that influences polar vortex strength is a potential source of intermittency (including internal variability, anthropogenic forcing, tropical variability, etc.), but we focus the discussion on factors that are most directly related to our CEN results.

To be more concrete, the intermittency of the stratospheric pathway stems from the fact that it can be reinforced or interrupted by other processes. For example, reinforcement can come from tropospheric pathways also detected by the CEN algorithm (see Fig. S1a and S1b):

1) $\downarrow \mathrm{ICE}_{\mathrm{Oct}} \Rightarrow \uparrow \mathrm{THF}_{\mathrm{Nov}} \Rightarrow \uparrow \mathrm{URALS}_{\mathrm{Jan}} \Rightarrow \uparrow \mathrm{URALS}_{\mathrm{Feb}} \Rightarrow \downarrow \mathrm{NAO}_{\mathrm{Mar}}$

2) $\downarrow \mathrm{ICE}_{\mathrm{Jan}} \Rightarrow \uparrow \mathrm{URALS}_{\mathrm{Feb}} \Rightarrow \downarrow \mathrm{NAO}_{\mathrm{Mar}}$

3) $\downarrow \mathrm{ICE}_{\mathrm{Nov}} \Rightarrow \downarrow \mathrm{NAO}_{\mathrm{Jan}}$

4) $\downarrow \mathrm{ICE}_{\mathrm{Jan}} \Rightarrow \downarrow \mathrm{NAO}_{\mathrm{Mar}}$

All these tropospheric and stratospheric pathways lead from the reduction of sea ice to a negative NAO, although they differ slightly in timing. The existence of the tropospheric pathway is supported by sea ice and surface heating perturbation experiments, where negative NAO/AO responses are simulated even when the stratospheric pathway is suppressed (Wu and Smith, 2016) or not well represented (Sun et al., 2015). However, the NAO/AO response is stronger when the stratospheric pathway is active than when it emerges through the tropospheric pathway alone (Nakamura et al., 2016; Zhang et al., 2018a, b).

Another example of a factor that may contribute to intermittency is the El Niño Southern Oscillation (ENSO). El Niño winters are associated with a deepened Aleutian low, which enhances upward propagating waves, weakens the polar vortex, and favours negative NAO conditions (Domeisen et al., 2019). As such, the stratospheric pathway may be reinforced if an El Niño develops following a low autumn ice season (both are associated with a weakened polar vortex, e.g., winter 1986/87 or 2009/10, Fig. 8); if a La Niña develops instead, the stratospheric pathway may be weakened (e.g., winter 2007/08 or 2010/11, Fig. 8). However, the relationship between wintertime ENSO and the NAO is rather weak (Brönnimann, 2007; Domeisen et al., 2019), consistent with Fig. 8, which shows high and low Nino3.4 values in both the lower (negative NAO) and upper (positive NAO) quadrants of the scatterplot. Given that we find no systematic phasing of ENSO with Barents-Kara sea ice variability during the reanalysis period, it is likely that ENSO contributes to intermittency in the ICE-NAO pathway.

In terms of reinforcing the stratospheric pathway, blocking over the Urals region seems to play a particularly important, but not fully understood, role. Enhanced Urals sea level pressure is closely linked to the Scandinavian pattern in Euro-Atlantic climate variability and is related, but not directly equivalent, to the occurrence of atmospheric blocking. The Urals linkage appears in the monthly CEN ($\downarrow \mathrm{ICE}_{\mathrm{Oct}} \Rightarrow \uparrow \mathrm{URALS}_{\mathrm{Dec}} \Rightarrow \uparrow \mathrm{V^*T^*}_{\mathrm{Dec/Jan}}$ in Fig. 3a). The latter segment from Urals sea level pressure to poleward eddy heat flux is fairly systematic (appears in 74% of the bootstrap samples in Fig. 5) and is grounded in the idea that tropospheric precursors over the Urals lead polar vortex weakening (Cohen and Jones, 2011; Cohen et al., 2014a). However, the first segment from Barents-Kara sea ice to Urals blocking is more intermittent (appears in 50% of the bootstrap samples), and whether it is in fact a causal linkage has been questioned by a recent modelling study using ensemble nudging experiments (Peings, 2019). Interestingly, not only Barents-Kara sea ice (Fig. 5e in King et al. (2016)) but also ENSO (Figs 5e and 5f in King et al. (2018)) has been linked to the Scandinavian pattern, which suggests another avenue for ENSO to contribute to intermittency.

The ICE-URALS relationship highlights the complexity of interactions between atmospheric internal variability and Barents-Kara sea ice over a range of time scales. On synoptic scales, the pentad CEN (Fig. 7) shows linkages from reduced sea ice to enhanced Urals sea level pressure, but also linkages in the opposite direction ($\uparrow$ URALS $\Rightarrow\uparrow$ IR $\Rightarrow\downarrow$ ICE), with Urals sea level pressure altering ice cover via changes in poleward moisture transport that have been tied to synoptic moist intrusions (Woods et al., 2013; Luo et al., 2016; Gong and Luo, 2017; Lee et al., 2017). This chain of linkages can act as a positive feedback on sea ice perturbations, but also provides a pathway by which blocking variability (internal to the atmosphere) may interrupt the expected troposphere-stratosphere coupling in response to autumn sea ice (for example, imagine a case where atmospheric conditions inhibit Urals blocking after a low-ice autumn). Furthermore, enhanced Urals blocking and moist intrusions can lead to highly transient perturbations in turbulent heat flux over the Barents-Kara Seas. Initially, turbulent heat loss from the ocean is suppressed near the sea ice edge where moist intrusions act to weaken temperature and moisture contrasts between the atmosphere and ocean (Woods et al., 2013; Gong and Luo, 2017). But the heat flux anomaly can become positive (enhanced heat loss from the ocean) after the sea ice melts back in response to the moist intrusion, one to two weeks later (Woods and Caballero, 2016; Lee et al., 2017). On longer (monthly to seasonal) time scales, there is evidence that atmospheric variability is the main driver of heat flux variability over the Barents-Kara Seas both in observations and models (Sorokina et al., 2016; Blackport et al., 2019). This perhaps explains why turbulent heat flux does not show up in the monthly CEN (Fig. 3a), but does in the half-monthly CEN (Fig. 3b). Across synoptic to seasonal timescales, it appears that sea ice is best thought of as an intermediary rather than a true boundary forcing, as is implied by prescribed sea ice (e.g., AGCM) experiments.

One outstanding issue involves the mechanisms that have been proposed to explain the $\downarrow \mathrm{ICE}_{\mathrm{Oct}} \Rightarrow\uparrow \mathrm{URALS}_{\mathrm{Dec}}$ linkage, which act on time scales that are inconsistent with the 2-month delay found in observations. For example, reduced sea ice may allow more heating of the atmosphere by the ocean to produce a Rossby wave train with an anomalous high over the Urals region (Honda et al., 2009), but this would be expected to manifest within a matter of days to a week. Alternatively, reduced ice may reduce local baroclinicity, which discourages cyclones from tracking into the Barents-Kara Seas and produces an anomalous high due to the relative absence of low-pressure systems (Inoue et al., 2012). This mechanism could introduce some delay between the ice perturbation and sea level pressure perturbation, but two months persistence of such a pattern is unlikely. Finally, reduced ice may increase atmospheric moisture content, leading to increased Eurasian snow cover, diabatic cooling and anomalously high sea level pressure over the continent (Liu et al., 2012; Cohen et al., 2014a; Garcia-Serrano and Frankignoul, 2014). Though this would plausibly lead to persistence on the required time scale, recent observational and modelling studies do not support a role for Eurasian snow in this teleconnection pathway (Kretschmer et al., 2016; Peings et al., 2017; Henderson et al., 2018), and we chose not to include it in our main analyses. Note that these mechanisms may still be responsible for contemporaneous forcing of the winter atmospheric circulation by winter sea ice variability, which has been suggested to be a stronger influence than the forcing by autumn sea ice variability (Blackport and Screen, 2019).

Lastly, our experience with the CEN offers some cautionary notes about its application to climate problems. The CEN approach was designed for hypothesis testing - that is, to test causal pathways that are thought or known to exist, either from theory or existing evidence. It should not be used as an exploratory data analysis tool to search for causal pathways because the statistics behind the CEN do not know whether relationships are physically meaningful. One specific problem we encountered is that the algorithm may drop an existing causal linkage if a new variable is added because of changes in the results of the partial correlations tests (see section 2.2). For example, when we introduce downward longwave radiation into the monthly CEN, its strong correlation with sea ice overrides the $\downarrow \mathrm{ICE}_{\mathrm{Jan}} \Rightarrow \uparrow \mathrm{URALS}_{\mathrm{Feb}}$ linkage (see Fig. S9 compared to Fig. S1a). Since many climate variables are highly correlated, but not necessarily directly related via specific processes, the CEN's ability to identify physically meaningful linkages depends critically on the careful selection of input variables.

5 Concluding remarks

This study uses the Causal Effect Networks (CEN) framework to quantify the robustness of the stratospheric pathway between late autumn Barents-Kara sea ice and the February NAO, documenting its high level of intermittency in the observational record. The pathway has been relatively "active" over the satellite period, explaining approximately 26% of the interannual variability in the February NAO. However, this result is highly sensitive to which winters are included in the analysis. Results from a bootstrapping test show that the full stratospheric pathway appears in only 16% of the sample populations derived from the observations. The result reflects the strong internal variability of the midlatitude atmosphere and the likelihood that Arctic-midlatitude teleconnections may require certain background flow conditions. On synoptic time scales, we identify two-way interactions between Barents-Kara sea ice and the midlatitude circulation suggesting a role for atmospheric blocking over the Urals region and moist intrusions, both of which can reduce Barents-Kara sea ice. These synoptic processes can reinforce or interrupt the stratospheric pathway, contributing to intermittency. Finally, we cannot rule out that the causal linkages found on longer time scales may be artefacts of averaging over the synoptic processes, or even the result of entirely different mechanisms (Smith et al., 2017; Hell et al., 2019).

Coupled interactions between sea ice and the midlatitude circulation involve complicated lead-lag feedbacks over a range of time scales. Applying causal inference frameworks such as the CEN can help clarify some of the important physical processes at play, but in the end, models are required to improve our understanding. A complication is that the fidelity of climate models in representing the relevant processes is difficult to ascertain (King et al., 2016; Smith et al., 2017; Mori et al., 2019), especially those processes at fine spatial and temporal scales and their interactions across scales. But ways forward are indicated by this study, along with others (McCusker et al., 2016; Sun et al., 2016; Peings, 2019), that provide insight into which linkages are most robust, and which are subject to sampling issues within the relatively short observational record.

Code availability. The codes to construct the CEN and figures in this study are available online at: https://github.com/petersiew/CEN

Data availability. ERA-Interim data are provided by European Centre for Medium-Range Weather Forecasts (ECMWF) online at :https://www.ecmwf.int/en/forecasts/datasets/reanalysis-datasets/era-interim

Author contributions. PS conducted the analysis, prepared the figures, and wrote the paper with contributions from all co-authors. CL and SPS conceived of the original idea. CL, SPS and MPK provided guidance on the interpretation of results.

Competing interests. Camille Li is a member of the editorial board of the journal.

Acknowledgements. This work was supported by the Research Council of Norway projects 255027 (DynAMiTe) and 272721 (Nansen Legacy). We acknowledge the European Centre for Medium-Range Weather Forecasts for providing the ERA-Interim data. Finally, we thank all members of the Bjerknes storm tracks group for stimulating discussions that helped improve this study.

References

Baldwin, M. P. and Dunkerton, T. J.: Propagation of the Arctic Oscillation from the stratosphere to the troposphere, Journal of Geophysical Research: Atmospheres, 104, 30 937–30 946, 1999.

Blackport, R. and Screen, J. A.: Influence of Arctic Sea Ice Loss in Autumn Compared to That in Winter on the Atmospheric Circulation, Geophysical Research Letters, 46, 2213–2221, 2019.

Blackport, R., Screen, J. A., van der Wiel, K., and Bintanja, R.: Minimal influence of reduced Arctic sea ice on coincident cold winters in mid-latitudes, Nature Climate Change, 9, 697–704, 2019.

Boisvert, L. N., Petty, A. A., and Stroeve, J. C.: The impact of the extreme winter 2015/16 Arctic cyclone on the Barents–Kara Seas, Monthly Weather Review, 144, 4279–4287, 2016.

Brönnimann, S.: Impact of El Niño–southern oscillation on European climate, Reviews of Geophysics, 45, 2007.

Cassano, E. N., Cassano, J. J., Higgins, M. E., and Serreze, M. C.: Atmospheric impacts of an Arctic sea ice minimum as seen in the Community Atmosphere Model, International Journal of Climatology, 34, 766–779, 2014.

Cavalieri, D. J. and Parkinson, C. L.: Arctic sea ice variability and trends, 1979-2010, The Cryosphere, 6, 881, 2012.

Charney, J. G. and Drazin, P. G.: Propagation of planetary-scale disturbances from the lower into the upper atmosphere, Journal of Geophysical Research, 66, 83–109, 1961.

Chen, H. W., Zhang, F., and Alley, R. B.: The robustness of midlatitude weather pattern changes due to Arctic sea ice loss, Journal of Climate, 29, 7831–7849, 2016.

Chen, X., Luo, D., Feldstein, S. B., and Lee, S.: Impact of winter Ural blocking on Arctic sea ice: short-time variability, Journal of Climate, 31, 2267–2282, 2018.

Cohen, J. and Jones, J.: Tropospheric precursors and stratospheric warmings, Journal of climate, 24, 6562–6572, 2011.

Cohen, J., Furtado, J. C., Jones, J., Barlow, M., Whittleston, D., and Entekhabi, D.: Linking Siberian snow cover to precursors of stratospheric variability, Journal of Climate, 27, 5422–5432, 2014a.

Cohen, J., Zhang, X., Francis, J., Jung, T., Kwok, R., Overland, J., Tayler, P., Lee, S., Laliberte, F., Feldstein, S., et al.: Arctic change and possible influence on mid-latitude climate and weather, US CLIVAR Report, 1, 2018.

Cohen, J., Zhang, X., Francis, J., Jung, T., Kwok, R., Overland, J., Ballinger, T., Bhatt, U., Chen, H., Coumou, D., et al.: Divergent consensuses on Arctic amplification influence on midlatitude severe winter weather, Nature Climate Change, pp. 1–10, 2019.

De, B. and Wu, Y.: Robustness of the stratospheric pathway in linking the Barents-Kara Sea sea ice variability to the mid-latitude circulation in CMIP5 models, Climate Dynamics, pp. 1–15, 2018.

Dee, D. P., Uppala, S., Simmons, A., Berrisford, P., Poli, P., Kobayashi, S., Andrae, U., Balmaseda, M., Balsamo, G., Bauer, d. P., et al.: The ERA-Interim reanalysis: Configuration and performance of the data assimilation system, Quarterly Journal of the royal meteorological society, 137, 553–597, 2011.

Deser, C., Walsh, J. E., and Timlin, M. S.: Arctic sea ice variability in the context of recent atmospheric circulation trends, Journal of Climate, 13, 617–633, 2000.

Deser, C., Magnusdottir, G., Saravanan, R., and Phillips, A.: The effects of North Atlantic SST and sea ice anomalies on the winter circulation in CCM3. Part II: Direct and indirect components of the response, Journal of Climate, 17, 877–889, 2004.

Deser, C., Tomas, R., Alexander, M., and Lawrence, D.: The seasonal atmospheric response to projected Arctic sea ice loss in the late twenty-first century, Journal of Climate, 23, 333–351, 2010.

Domeisen, D. I., Garfinkel, C. I., and Butler, A. H.: The teleconnection of El Niño Southern Oscillation to the stratosphere, Reviews of Geophysics, 57, 5–47, 2019.

Ebert-Uphoff, I. and Deng, Y.: Causal discovery for climate research using graphical models, Journal of Climate, 25, 5648–5665, 2012.

Fang, Z. and Wallace, J. M.: Arctic sea ice variability on a timescale of weeks and its relation to atmospheric forcing, Journal of Climate, 7, 1897–1914, 1994.

Francis, J. A.: Why are Arctic linkages to extreme weather still up in the air?, Bulletin of the American Meteorological Society, 98, 2551–2557, 2017.

Garcia-Serrano, J. and Frankignoul, C.: Retraction: High predictability of the winter Euro–Atlantic climate from cryospheric variability, 2014.

García-Serrano, J., Frankignoul, C., Gastineau, G., and De La Càmara, A.: On the predictability of the winter Euro-Atlantic climate: lagged influence of autumn Arctic sea ice, Journal of Climate, 28, 5195–5216, 2015.

Garfinkel, C. I., Hartmann, D. L., and Sassi, F.: Tropospheric precursors of anomalous Northern Hemisphere stratospheric polar vortices, Journal of Climate, 23, 3282–3299, 2010.

Gong, T. and Luo, D.: Ural blocking as an amplifier of the Arctic sea ice decline in winter, Journal of Climate, 30, 2639–2654, 2017.

Hall, R. J., Scaife, A. A., Hanna, E., Jones, J. M., and Erdélyi, R.: Simple statistical probabilistic forecasts of the winter NAO, Weather and Forecasting, 32, 1585–1601, 2017.

Hell, M. C., Schneider, T., and Li, C.: Atmospheric Circulation Response to Short-Term Arctic Warming in an Idealized Model, Journal of the Atmospheric Sciences, 2019.

Henderson, G. R., Peings, Y., Furtado, J. C., and Kushner, P. J.: Snow–atmosphere coupling in the Northern Hemisphere, Nature Climate Change, 8, 954–963, 2018.

Honda, M., Inoue, J., and Yamane, S.: Influence of low Arctic sea-ice minima on anomalously cold Eurasian winters, Geophysical Research Letters, 36, 2009.

Hopsch, S., Cohen, J., and Dethloff, K.: Analysis of a link between fall Arctic sea ice concentration and atmospheric patterns in the following winter, Tellus A: Dynamic Meteorology and Oceanography, 64, 18 624, 2012.

Hoshi, K., Ukita, J., Honda, M., Iwamoto, K., Nakamura, T., Yamazaki, K., Dethloff, K., Jaiser, R., and Handorf, D.: Poleward eddy heat flux anomalies associated with recent Arctic sea ice loss, Geophysical Research Letters, 44, 446–454, 2017.

Hurrell, J. W.: Decadal trends in the North Atlantic Oscillation: regional temperatures and precipitation, Science, 269, 676–679, 1995.

Inoue, J., Hori, M. E., and Takaya, K.: The role of Barents Sea ice in the wintertime cyclone track and emergence of a warm-Arctic cold-Siberian anomaly, Journal of Climate, 25, 2561–2568, 2012.

Jaiser, R., Nakamura, T., Handorf, D., Dethloff, K., Ukita, J., and Yamazaki, K.: Atmospheric winter response to Arctic sea ice changes in reanalysis data and model simulations, Journal of Geophysical Research: Atmospheres, 121, 7564–7577, 2016.

Karpechko, A. Y., Hitchcock, P., Peters, D. H., and Schneidereit, A.: Predictability of downward propagation of major sudden stratospheric warmings, Quarterly Journal of the Royal Meteorological Society, 143, 1459–1470, 2017.

Kim, B.-M., Son, S.-W., Min, S.-K., Jeong, J.-H., Kim, S.-J., Zhang, X., Shim, T., and Yoon, J.-H.: Weakening of the stratospheric polar vortex by Arctic sea-ice loss, Nature communications, 5, 4646, 2014.

Kim, B.-M., Hong, J.-Y., Jun, S.-Y., Zhang, X., Kwon, H., Kim, S.-J., Kim, J.-H., Kim, S.-W., and Kim, H.-K.: Major cause of unprecedented Arctic warming in January 2016: Critical role of an Atlantic windstorm, Scientific reports, 7, 40 051, 2017.

Kim, H.-M. and Kim, B.-M.: Relative contributions of atmospheric energy transport and sea ice loss to the recent warm Arctic winter, Journal of Climate, 30, 7441–7450, 2017.

King, M. P., Hell, M., and Keenlyside, N.: Investigation of the atmospheric mechanisms related to the autumn sea ice and winter circulation link in the Northern Hemisphere, Climate dynamics, 46, 1185–1195, 2016.

King, M. P., Herceg-Bulić, I., Bladé, I., García-Serrano, J., Keenlyside, N., Kucharski, F., Li, C., and Sobolowski, S.: Importance of late fall ENSO teleconnection in the Euro-Atlantic sector, Bulletin of the American Meteorological Society, 99, 1337–1343, 2018.

Koenigk, T., Caian, M., Nikulin, G., and Schimanke, S.: Regional Arctic sea ice variations as predictor for winter climate conditions, Climate Dynamics, 46, 317–337, 2016.

Kolstad, E. and Screen, J.: Non-Stationary Relationship between Autumn Arctic Sea Ice and the Winter North Atlantic Oscillation, Geophysical Research Letters, 2019.

Kretschmer, M., Coumou, D., Donges, J. F., and Runge, J.: Using causal effect networks to analyze different Arctic drivers of midlatitude winter circulation, Journal of Climate, 29, 4069–4081, 2016.

Kretschmer, M., Cohen, J., Matthias, V., Runge, J., and Coumou, D.: The different stratospheric influence on cold-extremes in Eurasia and North America, npj Climate and Atmospheric Science, 1, 1–10, 2018.

Kvamstø, N. G., Skeie, P., and Stephenson, D. B.: Impact of Labrador sea-ice extent on the North Atlantic Oscillation, International Journal of Climatology: A Journal of the Royal Meteorological Society, 24, 603–612, 2004.

Labe, Z., Peings, Y., and Magnusdottir, G.: The Effect of QBO Phase on the Atmospheric Response to Projected Arctic Sea Ice Loss in Early Winter, Geophysical Research Letters, 46, 7663–7671, 2019.

Lee, S., Gong, T., Feldstein, S. B., Screen, J. A., and Simmonds, I.: Revisiting the cause of the 1989–2009 Arctic surface warming using the surface energy budget: downward infrared radiation dominates the surface fluxes, Geophysical research letters, 44, 10–654, 2017.

Liptak, J. and Strong, C.: The winter atmospheric response to sea ice anomalies in the Barents Sea, Journal of Climate, 27, 914–924, 2014.

Liu, J., Curry, J. A., Wang, H., Song, M., and Horton, R. M.: Impact of declining Arctic sea ice on winter snowfall, Proceedings of the National Academy of Sciences, 109, 4074–4079, 2012.

Luo, B., Luo, D., Wu, L., Zhong, L., and Simmonds, I.: Atmospheric circulation patterns which promote winter Arctic sea ice decline, Environmental Research Letters, 12, 054 017, 2017.

Luo, D., Xiao, Y., Diao, Y., Dai, A., Franzke, C. L., and Simmonds, I.: Impact of Ural blocking on winter warm Arctic–cold Eurasian anomalies. Part II: The link to the North Atlantic Oscillation, Journal of Climate, 29, 3949–3971, 2016.

Magnusdottir, G., Deser, C., and Saravanan, R.: The effects of North Atlantic SST and sea ice anomalies on the winter circulation in CCM3. Part I: Main features and storm track characteristics of the response, Journal of Climate, 17, 857–876, 2004.

McCusker, K. E., Fyfe, J. C., and Sigmond, M.: Twenty-five winters of unexpected Eurasian cooling unlikely due to Arctic sea-ice loss, Nature Geoscience, 9, 838, 2016.

McKenna, C. M., Bracegirdle, T. J., Shuckburgh, E. F., Haynes, P. H., and Joshi, M. M.: Arctic sea ice loss in different regions leads to contrasting Northern Hemisphere impacts, Geophysical Research Letters, 45, 945–954, 2018.

Mori, M., Watanabe, M., Shiogama, H., Inoue, J., and Kimoto, M.: Robust Arctic sea-ice influence on the frequent Eurasian cold winters in past decades, Nature Geoscience, 7, 869, 2014.

Mori, M., Kosaka, Y., Watanabe, M., Nakamura, H., and Kimoto, M.: A reconciled estimate of the influence of Arctic sea-ice loss on recent Eurasian cooling, Nature Climate Change, 9, 123, 2019.

Nakamura, T., Yamazaki, K., Iwamoto, K., Honda, M., Miyoshi, Y., Ogawa, Y., and Ukita, J.: A negative phase shift of the winter AO/NAO due to the recent Arctic sea-ice reduction in late autumn, Journal of Geophysical Research: Atmospheres, 120, 3209–3227, 2015.

Nakamura, T., Yamazaki, K., Iwamoto, K., Honda, M., Miyoshi, Y., Ogawa, Y., Tomikawa, Y., and Ukita, J.: The stratospheric pathway for Arctic impacts on midlatitude climate, Geophysical Research Letters, 43, 3494–3501, 2016.

Nishii, K., Nakamura, H., and Miyasaka, T.: Modulations in the planetary wave field induced by upward-propagating Rossby wave packets prior to stratospheric sudden warming events: A case-study, Quarterly Journal of the Royal Meteorological Society: A journal of the atmospheric sciences, applied meteorology and physical oceanography, 135, 39–52, 2009.

Ogawa, F., Keenlyside, N., Gao, Y., Koenigk, T., Yang, S., Suo, L., Wang, T., Gastineau, G., Nakamura, T., Cheung, H. N., et al.: Evaluating impacts of recent Arctic sea ice loss on the northern hemisphere winter climate change, Geophysical Research Letters, 45, 3255–3263, 2018.

Onarheim, I. H. and Årthun, M.: Toward an ice-free Barents Sea, Geophysical Research Letters, 44, 8387–8395, 2017.

Orsolini, Y. J., Senan, R., Benestad, R. E., and Melsom, A.: Autumn atmospheric response to the 2007 low Arctic sea ice extent in coupled ocean–atmosphere hindcasts, Climate dynamics, 38, 2437–2448, 2012.

Outten, S. and Esau, I.: A link between Arctic sea ice and recent cooling trends over Eurasia, Climatic Change, 110, 1069–1075, 2012.

Overland, J. E. and Wang, M.: Arctic-midlatitude weather linkages in North America, Polar Science, 16, 1–9, 2018.

Overland, J. E., Dethloff, K., Francis, J. A., Hall, R. J., Hanna, E., Kim, S.-J., Screen, J. A., Shepherd, T. G., and Vihma, T.: Nonlinear response of mid-latitude weather to the changing Arctic, Nature Climate Change, 6, 992, 2016.

Park, D.-S. R., Lee, S., and Feldstein, S. B.: Attribution of the recent winter sea ice decline over the Atlantic sector of the Arctic Ocean, Journal of climate, 28, 4027–4033, 2015a.

Park, H.-S., Lee, S., Son, S.-W., Feldstein, S. B., and Kosaka, Y.: The impact of poleward moisture and sensible heat flux on Arctic winter sea ice variability, Journal of Climate, 28, 5030–5040, 2015b.

Peings, Y.: Ural Blocking as a Driver of Early-Winter Stratospheric Warmings, Geophysical Research Letters, 46, 5460–5468, 2019.

Peings, Y. and Magnusdottir, G.: Response of the wintertime Northern Hemisphere atmospheric circulation to current and projected Arctic sea ice decline: A numerical study with CAM5, Journal of Climate, 27, 244–264, 2014.

Peings, Y., Douville, H., Colin, J., Martin, D. S., and Magnusdottir, G.: Snow–(N) AO teleconnection and its modulation by the Quasi-Biennial Oscillation, Journal of Climate, 30, 10 211–10 235, 2017.

Petoukhov, V. and Semenov, V. A.: A link between reduced Barents-Kara sea ice and cold winter extremes over northern continents, Journal of Geophysical Research: Atmospheres, 115, 2010.

Polvani, L. M. and Waugh, D. W.: Upward wave activity flux as a precursor to extreme stratospheric events and subsequent anomalous surface weather regimes, Journal of climate, 17, 3548–3554, 2004.

Runge, J., Petoukhov, V., and Kurths, J.: Quantifying the strength and delay of climatic interactions: The ambiguities of cross correlation and a novel measure based on graphical models, Journal of Climate, 27, 720–739, 2014.

Runge, J., Petoukhov, V., Donges, J. F., Hlinka, J., Jajcay, N., Vejmelka, M., Hartman, D., Marwan, N., Paluš, M., and Kurths, J.: Identifying causal gateways and mediators in complex spatio-temporal systems, Nature communications, 6, 1–10, 2015.

Runge, J., Nowack, P., Kretschmer, M., Flaxman, S., and Sejdinovic, D.: Detecting and quantifying causal associations in large nonlinear time series datasets, Science Advances, 5, eaau4996, 2019.

Scaife, A., Arribas, A., Blockley, E., Brookshaw, A., Clark, R., Dunstone, N., Eade, R., Fereday, D., Folland, C., Gordon, M., et al.: Skillful long-range prediction of European and North American winters, Geophysical Research Letters, 41, 2514–2519, 2014.

Screen, J. A.: Simulated atmospheric response to regional and pan-Arctic sea ice loss, Journal of Climate, 30, 3945–3962, 2017.

Screen, J. A., Deser, C., Simmonds, I., and Tomas, R.: Atmospheric impacts of Arctic sea-ice loss, 1979–2009: Separating forced change from atmospheric internal variability, Climate dynamics, 43, 333–344, 2014.

Screen, J. A., Deser, C., Smith, D. M., Zhang, X., Blackport, R., Kushner, P. J., Oudar, T., McCusker, K. E., and Sun, L.: Consistency and discrepancy in the atmospheric response to Arctic sea-ice loss across climate models, Nature Geoscience, p. 1, 2018.

Semenov, V. A. and Latif, M.: Nonlinear winter atmospheric circulation response to Arctic sea ice concentration anomalies for different periods during 1966–2012, Environmental Research Letters, 10, 054 020, 2015.

Serreze, M. C. and Stroeve, J.: Arctic sea ice trends, variability and implications for seasonal ice forecasting, Philosophical Transactions of the Royal Society A: Mathematical, Physical and Engineering Sciences, 373, 20140 159, 2015.

Shepherd, T. G.: Effects of a warming Arctic, Science, 353, 989–990, 2016.

Singarayer, J. S., Bamber, J. L., and Valdes, P. J.: Twenty-first-century climate impacts from a declining Arctic sea ice cover, Journal of Climate, 19, 1109–1125, 2006.

Smith, D. M., Dunstone, N. J., Scaife, A. A., Fiedler, E. K., Copsey, D., and Hardiman, S. C.: Atmospheric response to Arctic and Antarctic sea ice: The importance of ocean–atmosphere coupling and the background state, Journal of Climate, 30, 4547–4565, 2017.

Smith, D. M., Screen, J. A., Deser, C., Cohen, J., Fyfe, J. C., García-Serrano, J., Jung, T., Kattsov, V., Matei, D., Msadek, R., et al.: The Polar Amplification Model Intercomparison Project (PAMIP) contribution to CMIP6: investigating the causes and consequences of polar amplification, Geoscientific Model Development, 12, 1139–1164, 2019.

Smith, K. L., Fletcher, C. G., and Kushner, P. J.: The role of linear interference in the annular mode response to extratropical surface forcing, Journal of Climate, 23, 6036–6050, 2010.

Sorokina, S. A., Li, C., Wettstein, J. J., and Kvamstø, N. G.: Observed atmospheric coupling between Barents Sea ice and the warm-Arctic cold-Siberian anomaly pattern, Journal of Climate, 29, 495–511, 2016.

Strey, S. T., Chapman, W. L., and Walsh, J. E.: The 2007 sea ice minimum: Impacts on the Northern Hemisphere atmosphere in late autumn and early winter, Journal of Geophysical Research: Atmospheres, 115, 2010.

Strong, C., Magnusdottir, G., and Stern, H.: Observed feedback between winter sea ice and the North Atlantic Oscillation, Journal of Climate, 22, 6021–6032, 2009.

Sun, L., Deser, C., and Tomas, R. A.: Mechanisms of stratospheric and tropospheric circulation response to projected Arctic sea ice loss, Journal of Climate, 28, 7824–7845, 2015.

Sun, L., Perlwitz, J., and Hoerling, M.: What caused the recent “Warm Arctic, Cold Continents” trend pattern in winter temperatures?, Geophysical Research Letters, 43, 5345–5352, 2016.

Wang, L., Ting, M., and Kushner, P.: A robust empirical seasonal prediction of winter NAO and surface climate, Scientific reports, 7, 279, 2017.

Wickström, S., Jonassen, M., Vihma, T., and Uotila, P.: Trends in cyclones in the high-latitude North Atlantic during 1979–2016, Quarterly Journal of the Royal Meteorological Society, 2019.

Woods, C. and Caballero, R.: The role of moist intrusions in winter Arctic warming and sea ice decline, Journal of Climate, 29, 4473–4485, 2016.

Woods, C., Caballero, R., and Svensson, G.: Large-scale circulation associated with moisture intrusions into the Arctic during winter, Geophysical Research Letters, 40, 4717–4721, 2013.

Wu, Q. and Zhang, X.: Observed forcing-feedback processes between Northern Hemisphere atmospheric circulation and Arctic sea ice coverage, Journal of Geophysical Research: Atmospheres, 115, 2010.

Wu, Y. and Smith, K. L.: Response of Northern Hemisphere midlatitude circulation to Arctic amplification in a simple atmospheric general circulation model, Journal of Climate, 29, 2041–2058, 2016.

Yang, X.-Y., Yuan, X., and Ting, M.: Dynamical link between the Barents–Kara sea ice and the Arctic Oscillation, Journal of Climate, 29, 5103–5122, 2016.

Zhang, P., Wu, Y., and Smith, K. L.: Prolonged effect of the stratospheric pathway in linking Barents-Kara Sea sea ice variability to the midlatitude circulation in a simplified model, Climate Dynamics, 50, 527–539, 2018a.

Zhang, P., Wu, Y., Simpson, I. R., Smith, K. L., Zhang, X., De, B., and Callaghan, P.: A stratospheric pathway linking a colder Siberia to Barents-Kara Sea sea ice loss, Science advances, 4, eaat6025, 2018b.

Zhong, L., Hua, L., and Luo, D.: Local and external moisture sources for the Arctic warming over the Barents–Kara seas, Journal of Climate, 31, 1963–1982, 2018.

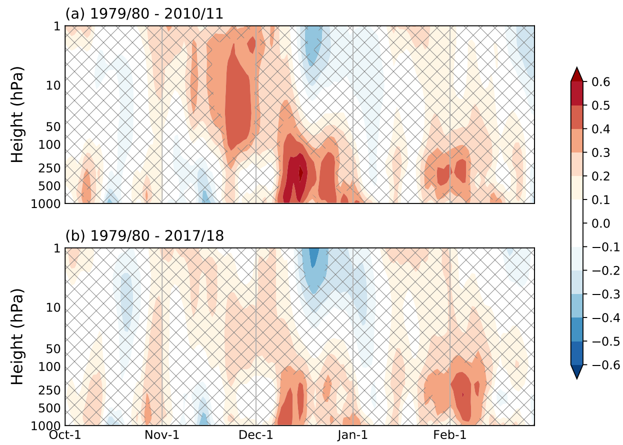

Figure 1. Lead-lag correlations (shading) between November Barents-Kara sea ice index (sign reversed) and polar cap height (70°N poleward) over the October-to-February cold season using ERA-Interim reanalysis for two periods: (a) 1979/80-2010/11 and (b) 1979/80-2017/18. Hatching indicates non-significant values at the 5% level using a two-tailed t-test. Linear trends and the seasonal cycle have been removed.

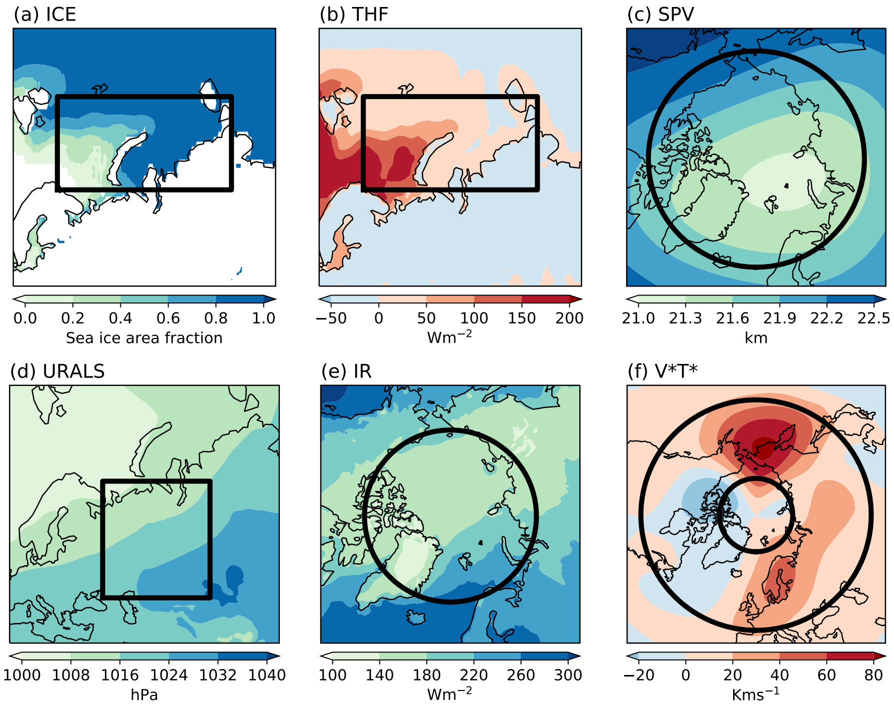

Figure 2. ERA-Interim (1979-2018) DJF climatologies (shading) of key variables and regions (black boxes) for computing area-averaged indices: (a) Sea ice area fraction, 70°-80° N, 30°-105° E, (b) Turbulent heat flux, 70°-80° N, 30°-105° E, (c) Stratospheric polar vortex, which is defined by 10-100 hPa geopotential height, 65°-90° N, (d) Urals sea level pressure, 45°-70° N, 40°-85° E, (e) Downward longwave radiation, 70°-90° N, (f) 100 hPa poleward eddy heat flux, 45°-75° N. For (b), turbulent heat flux from the ocean to the atmosphere is defined as positive. See section 2.1 for details.

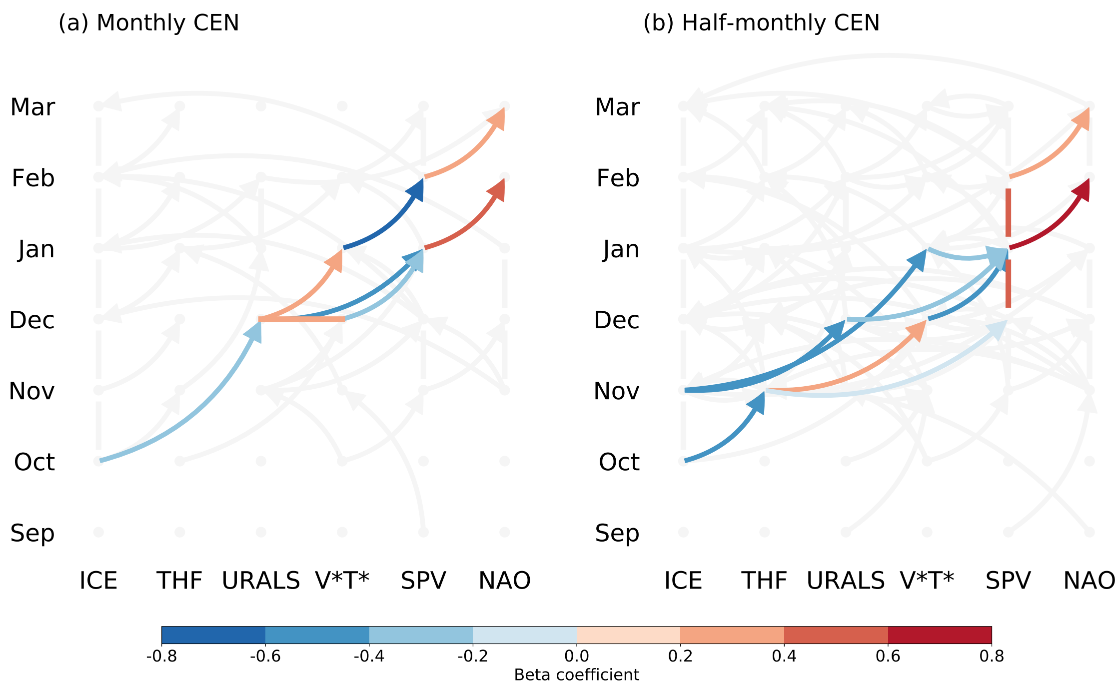

Figure 3. Seasonal evolution of the stratospheric pathway (indicated by coloured arrows) detected by the (a) monthly and (b) half-monthly CENs. Arrows indicate causal linkages; vertical lines indicate auto-correlation; horizontal bars indicate simultaneous relationships; colours show the sign and strength of the linkages as given by the CEN beta coefficients (see section 2.2). The grey background shows other significant linkages (arrows) and autocorrelations (vertical lines), but does not include simultaneous relationships. The half-monthly CEN in (b) has been aggregated into full months for ease of comparison with (a). See Fig. S2 for unaggregated version.

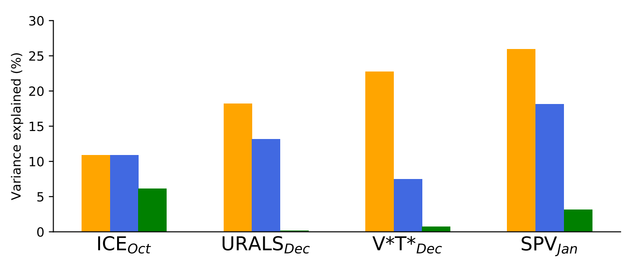

Figure 4. Explanatory power of the stratospheric pathway for the February NAO assessed via multiple linear regression. Orange bars show the cumulative variance explained when including each regressor in succession from left to right; blue bars show variance explained by the individual regressor; green bars show the reduction in total variance explained when removing that regressor. See section 3.2 for details.

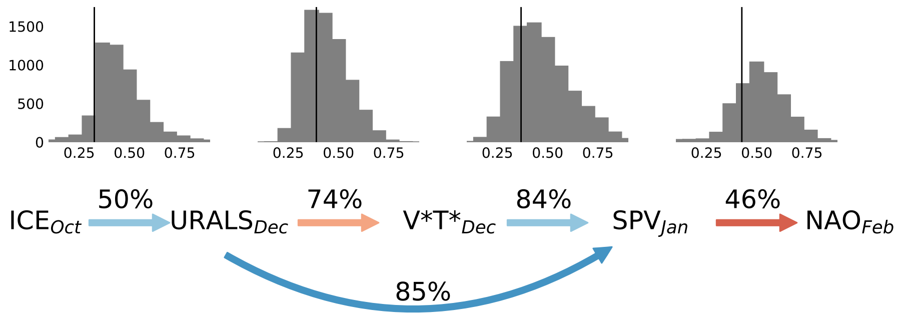

Figure 5. Results of a bootstrapping test to assess the robustness of causal linkages within the stratospheric pathway. Percentages above arrows show the occurrence rate of each linkage out of 10,000 bootstrap samples. Colours of the arrows (identical to Fig. 3) and the black lines show observed beta coefficients for each linkage for the reanalysis period. Histograms above show the corresponding distribution of beta coefficients (absolute value) in the bootstrap samples. The histogram for the $\uparrow \mathrm{URALS}_{\mathrm{Dec}} \Rightarrow \downarrow \mathrm{SPV}_{\mathrm{Jan}}$ linkage is not shown. Note that the distributions are composed only of samples in which the linkage is detected.

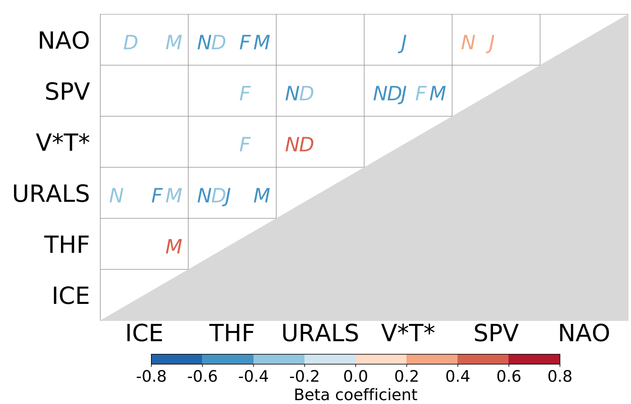

Figure 6. Simultaneous relationships between monthly indices in November (N), December (D), January (J), February (F) and March (M). Colours indicate the sign and strength of the relationship as given by the CEN beta coefficients (see section 2.2).

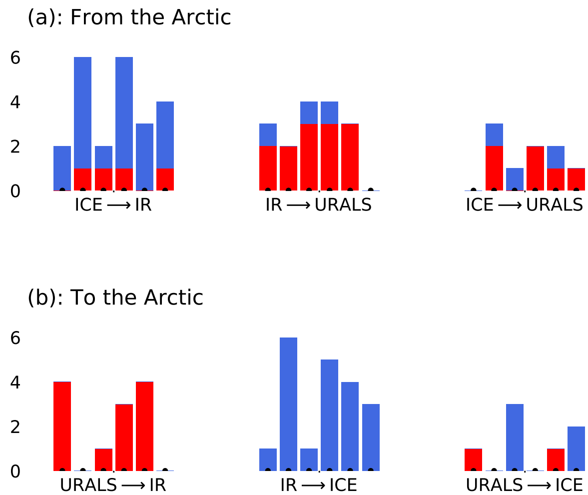

Figure 7. Results of the pentad CEN analysis assessing relationships between downward longwave radiation (IR), Barents-Kara sea ice (ICE) and Urals sea level pressure (URALS) aggregated into months (October, November, December, January, February and March from left to right). The height of each bar is the number of counts. (a) Linkages from the Arctic to the midlatitudes. (b) Linkages from the midlatitudes to the Arctic. Red (blue) colours denote positive (negative) relationships. See Fig. S8 for unaggregated version.

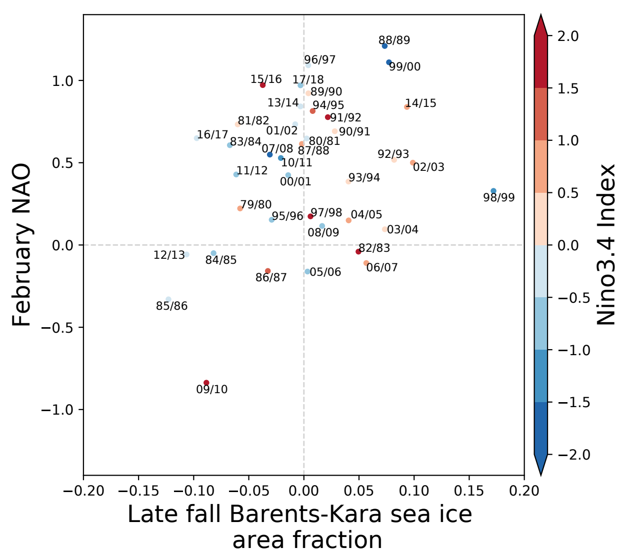

Figure 8. Scatter plots between February NAO and late fall (mean of October and November) Barents-Kara sea ice index for the reanalysis period. Shading indicates the DJF Nino3.4 index. Red (blue) denotes El Niño (La Niña) events.

Table 1. A summary of the casual effect of all ICE-NAO pathways. The $\downarrow \mathrm{ICE_{Oct}} \Rightarrow \downarrow \mathrm{NAO_{Mar}}$ pathway consists of both tropospheric and stratospheric branches.

Pathway	Tropospehric	Stratospheric	Total
$\downarrow \mathrm{ICE_{Oct}} \Rightarrow \downarrow \mathrm{NAO_{Feb}}$	N/A	0.0823	0.0823
$\downarrow \mathrm{ICE_{Oct}} \Rightarrow \downarrow \mathrm{NAO_{Mar}}$	0.0614 (70%)	0.0258 (30%)	0.0872
$\downarrow \mathrm{ICE_{Jan}} \Rightarrow \downarrow \mathrm{NAO_{Mar}}$	0.137	N/A	0.137